2018-12-01

Gut Microbiota Regulates the Interplay Between Diet and Genetics to Influence Insulin Resistance

Jeralyn Jones Franson
Brigham Young University

Gut Microbiota Regulates the Interplay Between Diet and Genetics to Influence Insulin Resistance

Jeralyn Jones Franson

A thesis submitted to the faculty of
Brigham Young University
in partial fulfillment of the requirements for the degree of

Master of Science

Laura Clarke Bridgewater, Chair
Mary Feller Davis
Julianne House Grose

Department of Microbiology and Molecular Biology

Brigham Young University

ABSTRACT

Gut Microbiota Regulates the Interplay Between Diet and Genetics to Influence Insulin Resistance

Jeralyn Jones Franson
Department of Microbiology and Molecular Biology, BYU
Master of Science

Insulin resistance and obesity are major public health concerns. The impact of diet and genetics on insulin resistance and obesity is well accepted. Additionally, the gut microbiota has been shown to influence obesity and metabolic disorders. However, much remains to be understood about the role of gut microbiota in the development of insulin resistance and obesity. We utilized a mouse model with a global deletion of PAS kinase, a protein involved in cellular metabolism, to better understand the relationship between diet, genetics and the gut microbiota. Previous research has shown that mutant mice, lacking PAS kinase, were protected from the effects of a high fat diet, gaining less weight and showing a better response to insulin than high fat diet fed wild-type mice. Surprisingly, when PAS-kinase knockout mice were placed on a western-style, high fat, high sugar (HFHS) diet, they became obese and had an impaired response to insulin, much like wild type mice on the same diet. Mutant mice did, however, show more resistance to the effects of the unhealthy diet in one aspect—they maintained normal levels of claudin-1 in the colon, suggesting that they were less likely to develop excessive gut permeability (leaky gut). While significant differences in gut microbial composition were seen in response to the HFHS diet, with shifts in the ratio of Firmicutes/Bacteroidetes and increases in the levels of Actinobacteria, none of the differences correlated with genotype. Unexpectedly, however, within the mice on the HFHS diet and regardless of genotype, the composition of the gut microbiota diverged into two clusters. The mice in one cluster showed more resistance to obesity and their glucose response was like that of wild type mice on a healthy normal chow diet (NCD), while mice in the other cluster showed more weight gain and impaired glucose response. No similar gut microbiota divergence occurred in mice on the NCD, suggesting that the HFHS diet made mice vulnerable to (but did not cause) the development of a harmful gut microbiota, whereas the healthy NCD protected against spontaneous harmful shifts in the composition of the gut microbiota.

Keywords: PAS-kinase, gut microbiota, western diet, metabolism, obesity, glucose tolerance

ACKNOWLEDGEMENTS

I would like to thank my committee, Dr. Laura Bridgewater, Dr. Mary Davis, and Dr. Julianne Grose for their support and suggestions for the duration of my research. I would like to especially thank Dr. Grose for her support and inspiration in pursing an advanced degree in molecular biology. I would also like to thank Dr. Mikle South for his support on my original project. I would like to thank the numerous members of the Bridgewater lab for their help and support in this project, particularly our lab managers Kaitlyn Williams and Haley Burrell, who provided help in maintaining the mouse colony as well as emotional support. I am grateful for the assistance of the Arroyo, Kooyman, and Hansen labs in all steps in the immunoblotting process, and to the Grose lab for support and troubleshooting experiments. I would like to thank Brandon Rose, Claudia Tellez Freitas, Deborah Johnson, and Kiara Whitley for their examples of excellence in science, and for their support, encouragement and ideas. I am grateful to Kiara particularly for her editing and reviewing suggestions. Finally, I would like to thank my sister for her constant support and encouragement and my family for their patience over the last four years as I have worked to achieve my dream.

TABLE OF CONTENTS

LIST OF TABLES

LIST OF FIGURES

Introduction

Obesity and Insulin Resistance

Insulin resistance and obesity are a major public health problem. Obesity affects 39.8 % of adults in the United States [1] (Figure 1) and its prevalence is increasing worldwide [2]. Body mass index (BMI) is calculated by dividing weight in kilograms by the square of height in meters, and obesity is defined as a BMI of 30 kg/m^2 or greater. Obesity often occurs alongside metabolic disease, which symptomatically manifests as elevated levels of fasting blood glucose, liver triglycerides and blood pressure, as well as lower levels of high-density lipoprotein [3]. Obesity can lead to type 2 diabetes, certain cancers, cardiovascular diseases, stroke, and non-alcoholic fatty liver disease [4-7].

In healthy individuals, increased blood glucose levels trigger beta cells in the pancreas to produce insulin. Extracellular insulin can subsequently bind to insulin receptors on cellular membranes [8], allowing for increased glucose uptake by the cell by translocating glucose receptors to the cellular membrane, and stimulating glycogen synthesis [9]. A decrease in the cell's sensitivity to insulin is known as insulin resistance, and it can then lead to hyperglycemia, hepatic lipid synthesis and adiposity [10]. The severity of insulin resistance is used to classify individuals as either prediabetes or type 2 diabetes. Prediabetes, which affects 33.9% of adults in the United States (Figure 1), involves a fasting blood glucose between 100-125mg/dL[11]. A fasting blood glucose above 125 mg/dL is indicative of type 2 diabetes, which has been diagnosed in 8.6% of adults in the US-(Figure 1) [11]. Of adults diagnosed with diabetes, 87.5% were overweight or obese [12].

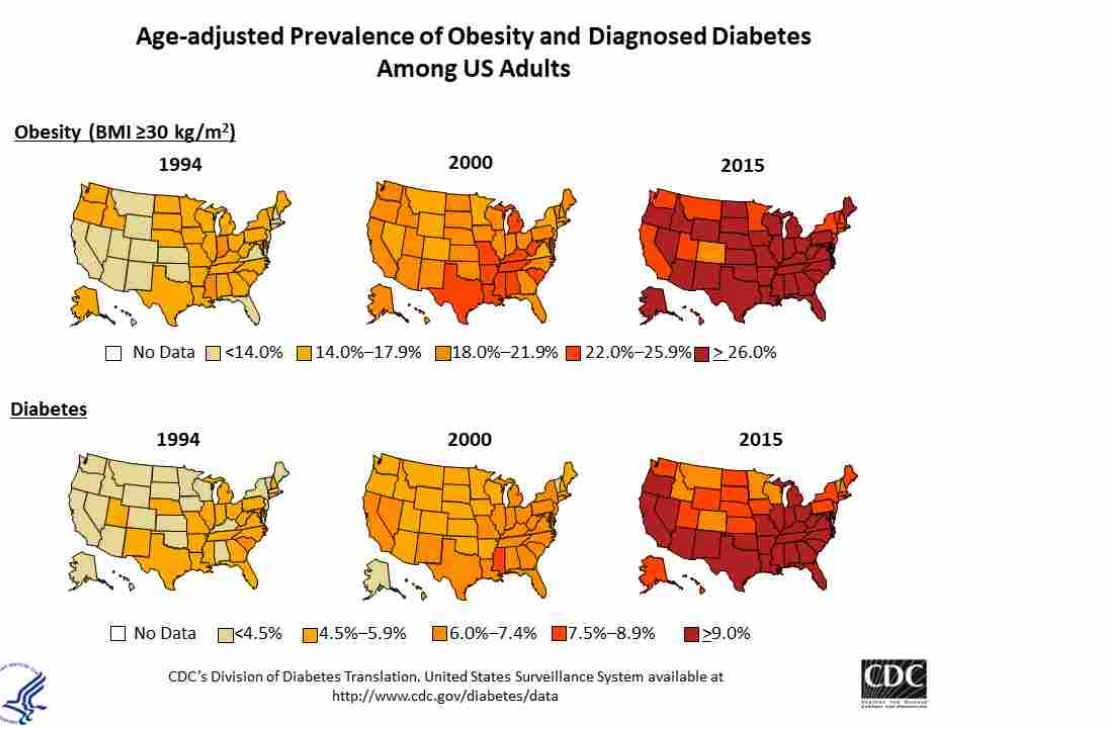

Figure 1. Growth rates of obesity and Diabetes in the United States. From National Diabetes Statistics Report, 2017. Centers for Disease Control and Prevention

Diet and the Gut Microbiota

Diet plays an important role in the development of obesity and insulin resistance. Adults in the United States consume 14.9% of their daily calories from sugar [13]. Overconsumption of sugars can lead to metabolic disease [14] and a high-fat diet is a significant driver in the development of obesity [15]. Between 2013 and 2016, 37% of adults in the United States ate fast food, typically high in fat, sugar and calories, on a given day [16].

In addition to over nutrition's caloric contribution to obesity, the influence of diet on obesity and insulin resistance can be traced through the direct effect diet has on the gut microbiota. The gut microbiota refers to the collection of microorganisms that inhabit the intestinal tract. Over 1000 bacterial species have been identified in the human intestine [17], with populations ranging from 10^3 bacterial cells/gram of tissue (bacteria/g) in the duodenum, 10^4 bacteria/g in the jejunum, 10^7 bacteria/g in the ileum and 10^{12} bacteria/g in the colon[18]. The

duodenum, jejunum and ileum have a higher prevalence of Firmicutes (Lactobacillacea family), Proteobacteria, and Actinobacteria, while the colon has a higher prevalence of Bacteroidetes, Firmicutes (Lachnospiraceae and Ruminococcaceae families), and Verrucomicrobia (*Akkermansia* genus)[18]. This diverse collection of bacteria exists in a delicate dance with the host, as the bacteria are influenced by immune cells and nutrients provided by the host, and the host's health is subsequently affected by the bacteria in a beneficial or detrimental manner.

Gut bacteria influence the host primarily through by-products of their metabolism. The gut microbiota is responsible for the breakdown of complex polysaccharides otherwise undigestible by the host. Conversion of complex polysaccharides into short chain fatty acids (SCFA) and fermentation in the colon supplies 10% of the host's daily energy requirements [19]. SCFA include acetate, a substrate for gluconeogenesis and lipogenesis, propionate, a regulator of immune function and intestinal physiology [19] and butyrate, a regulator of intestinal barriers [20]. The gut microbiota also plays a key role in the development and stimulation of immune function [21], with SCFA playing a key role in the communication between the host immune system and microbiota [22]. The gut microbiota is also the sole supplier of essential vitamins, including vitamins B and K [23].

The gut microbiota plays an important role in the development of obesity and insulin resistance. The link between obesity and the gut microbiota was first shown by Gordon et al [24], with shifts in the ratio of Bacteroidetes, a Gram-negative bacteria, and Firmicutes, a Gram-positive bacteria, in genetically obese mice. Further studies also showed a preponderance of Firmicutes in both obese human subjects [7] and high-fat fed mice [25]. Additionally, studies showed that transplantation of microbiota from obese human donors into germ-free mice led to the development of weight gain and insulin resistance [26-29]. Specific strains of bacteria isolated from

human hosts and transplanted into germ free mice were shown to induce the correlated phenotype (either lean or obese) found in the host. *Enterobacter cloacae* B29, isolated from the microbiota of an obese human patient (BMI 58.78 kg/m^2) , induced obesity when transferred into high-fat fed germ free mice, whereas germ free mice on the high fat diet that did not receive the B29 transfer remained lean. [27]. *Bifidobacterium pseudocatenulatum* C95, isolated from the gut bacteria of type 2 diabetes patients assigned a high-fiber diet and probiotics, is associated with improved hypoglycemia when transferred into high-fat fed germ free mice [30]. *Akkermansia muciniphila,* found in the gut microbiota of both humans and mice, is linked to improved glucose tolerance and body weight in both humans and mice [29,31,32].

The role of diet on the gut microbiota has been further elucidated through studies on germ free mice. Germ-free mice on a high-fat diet were protected from obesity and insulin resistance [33]. In conventional (not germ-free) mice, a high-fat diet alters the gut microbiota, and subsequent alteration of the microbiota through administration of oral antibiotics ameliorated the effects of a high-fat diet on weight gain, adiposity, glucose intolerance and inflammation [25]. A high-fat high-sugar diet (HFHS) also alters the gut microbiota, and it increases intestinal permeability [34]. However, germ-free mice fed a HFHS diet did not develop obesity or insulin resistance [26], suggesting a causal role for the gut microbiota in the development of diet-induced obesity and insulin resistance.

Intestinal Permeability

The exact mechanisms by which gut bacteria influence weight gain and insulin resistance are unknown but may be related to the inflammatory response triggered by lipopolysaccharide (LPS), an endotoxin from the cell walls of gram negative bacteria. Dietary sugar has been shown to lead to increased hepatic fat and translocation of LPS from the intestines into the bloodstream

of mice [35]. Elevated levels of circulating LPS are also correlated with obesity and insulin resistance [25,34]. LPS can pass through the intestinal epithelium into the bloodstream when tight junctions between epithelial cells are disrupted. Claudin-1, zonula occludens-1, and occludin are proteins in these epithelial barriers-which play a crucial role in the regulation of intestinal permeability [36]. A high-fat diet has been shown to increase intestinal permeability [25] and significantly decrease levels of tight junction proteins, including claudin [37].

Current research suggests the mechanism by which the gut microbiota influences levels of tight junction proteins is via the Protein Kinase B (Akt) signaling pathway. LPS from gram-negative bacteria binds to toll like receptor-4 on the surface of a cell, which triggers the production of inflammatory cytokines including tumor necrosis factor α (TNF-α) and NFκB [38,39]. In intestinal epithelial cells, NFκB activates inflammatory cytokines which inhibit the Akt/mTOR signaling pathway [20]. Inhibition of the Akt signaling pathway reduces levels of tight junction protein expression [40].

Metabolic markers

In adipose, muscle, and liver tissue, the phosphoinositide kinase (PI3K) PI3K/Akt signaling pathway plays a key role in metabolism and the development of type 2 diabetes and obesity [41]. Insulin secreted from the pancreas after eating activates the PI3K/AKT pathway (Figure 2). Akt is activated by phosphorylation first at threonine 308 [42], then at serine 473 by mTOR, through a PI3K-dependant mechanism [43]. When activated, Akt signals for translocation of glucose transporter 4 (GLUT4) to the cell membrane, allowing glucose uptake (42). Activated Akt ($pAkt^{ser473}$) also inhibits the insulin receptor substrate (IRS) [41]. Reduced levels of $pAkt^{ser473}$ are seen in mice fed a high-fat diet [44,45] and bama pigs fed a high-fat high-sugar diet [46]. In the

liver of normal chow diet fed mice, pAkt^{ser473} levels were overexpressed in mutants lacking Per-Arnt-Sim (PAS) kinase, a metabolic protein [47,48].

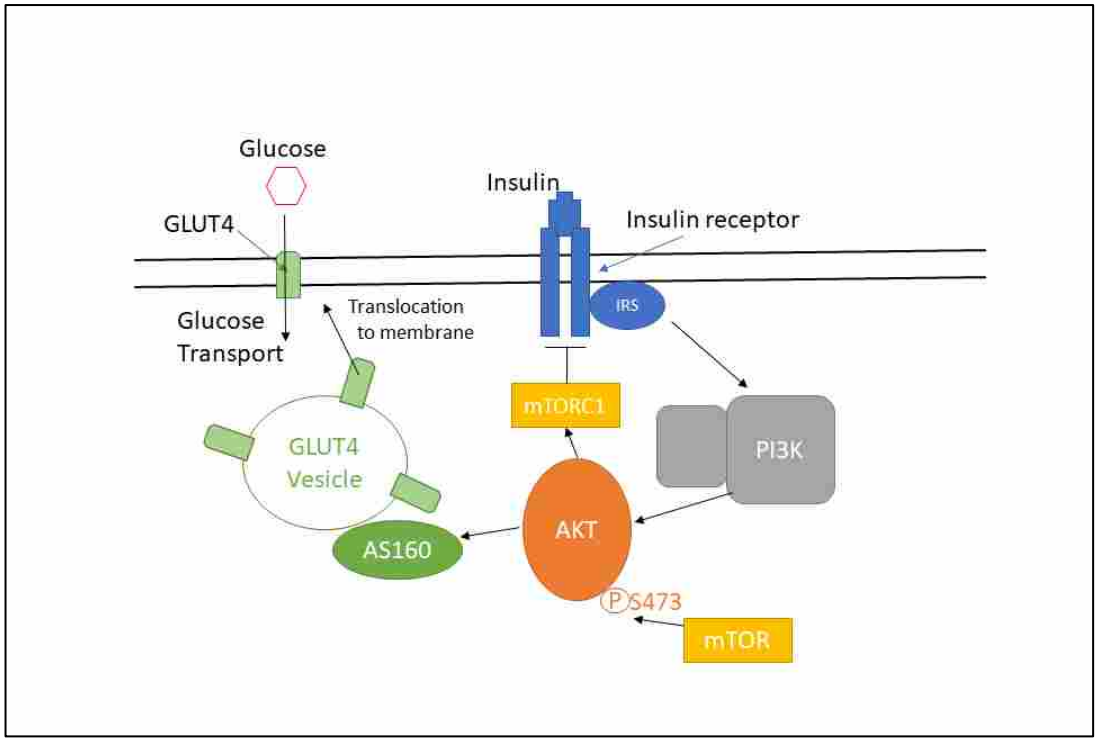

Figure 2. Overview of the metabolic pathways associated with Akt in muscle tissue.

Genetics

Per-Arnt-Sim kinase (PASK) is a protein involved in detecting the energy of the cell and regulating metabolism [49]. Previous research has shown that PASK knockout mice on a high fat diet were protected from insulin resistance and obesity and demonstrated increased cellular metabolism [50]. The exact role of PASK in the cell is still unknown, but it is thought to be closely involved with AMPK, insulin gene expression, and glucagon secretion [51,52]. In this research we examined the role that gut microbiota play in metabolic health and their ability to override genetic influences to induce obesity and insulin resistance.

Hypothesis

The original aim of this research project was to determine whether PASK-deficient mice would still be protected from weight gain and insulin resistance when placed on a Western diet--one high in both fats and sugars. We also wanted to analyze whether the gut bacteria of PASK-deficient mice would reflect diet or genotype. The role PASK may play in the composition of the gut microbiota had not been studied previously. We hypothesized that microbiota primarily contribute to any difference in glucose sensitivity by triggering systemic inflammation. This could occur if certain bacteria secrete metabolites that increase gut permeability, which would be reflected by reduced levels of claudin-1. Increased gut permeability should lead to LPS circulating in the blood as well as circulating cytokines. The subsequent inflammatory response will affect activation of Akt in the muscle, resulting in insulin resistance.

This research illuminated the role bacteria play in overriding genetics to influence metabolic health. Understanding this role, and the cellular response to inflammatory signals, could help us create better treatments and preventions for insulin resistance.

Study design

Animals

Housing: All procedures were carried out with the approval of the Institutional Animal Care and Use Committee (IACUC) of Brigham Young University (protocols 16-1003 and 13-1003). 2 male and 1 female PASK +/- mice were obtained from the Rutter lab 53 and bred to produce the colony used for this study. Upon weaning at 3 weeks of age, littermates were randomly assigned to either a normal chow diet (NCD) (8604; Tekland Diets, Madison, WI; protein 32% kcal, fat 14%, carbohydrate 54%) or a western-style high-fat, high-sugar diet (HFHS) (D12266Bi;

Research Diets, Inc., New Brunswick, NJ; protein 16.8% kcal, fat 31.8%, carbohydrate 51.4%). Mice were co-housed according to sex, genotype, and assigned diet. All mice were housed with no more than five mice per cage, on a 12-hour light/dark cycle. Water and food were freely available.

Genotyping*: PASK* genotypes were determined by genomic polymerase chain reaction (PCR) of tail snip specimens. Tails were digested in 100 µl lysis buffer (10 ml 1M Tris-HCl, pH 8.0, 1 ml .5 M EDTA, pH 8.0, 4ml 5 M NaCl, ddH_20 to 100ml) and 5 µl proteinase K overnight (14-16 hours) at 50 °C, shaking at 90-98 RPM. Samples were then boiled for 5 minutes and stored at 4°C. PCR was performed using 1µl ddH_20, 2.5 µl 10µM forward *PASK* primer (5'-GAAGTCACCCCCGATCCCCTCCTAAC-3'), 1.25 µl 10µM *PASK* MUT primer(5'-ACTTTCGGTTCCTCTTCCCATGAATTC-3'), 1.25ul 10µM *PASK* WT primer(5'-CTAGCCATGGTGCTTACCCTC-3'), 6.5 µl GoTaq GreenMaster Mix (Promega, Madison, WI), and 2 µl template DNA for a total volume of 14.5µl per sample. Lid 100°C, (94°C for 20seconds, 64°C for 30 seconds, 70°C for 35 seconds) x30. Hold at 4°C. Bands were checked on a 1.4% agarose gel using 6µl of PCR product (Figure 3).

Weekly weight and fecal collection: To track changes in weight and gut microbial contents, mice were weighed weekly and fecal samples were collected. Fecal samples were placed into a sterile, labeled Eppendorf tube and immediately placed on dry ice until storage at -80°C.

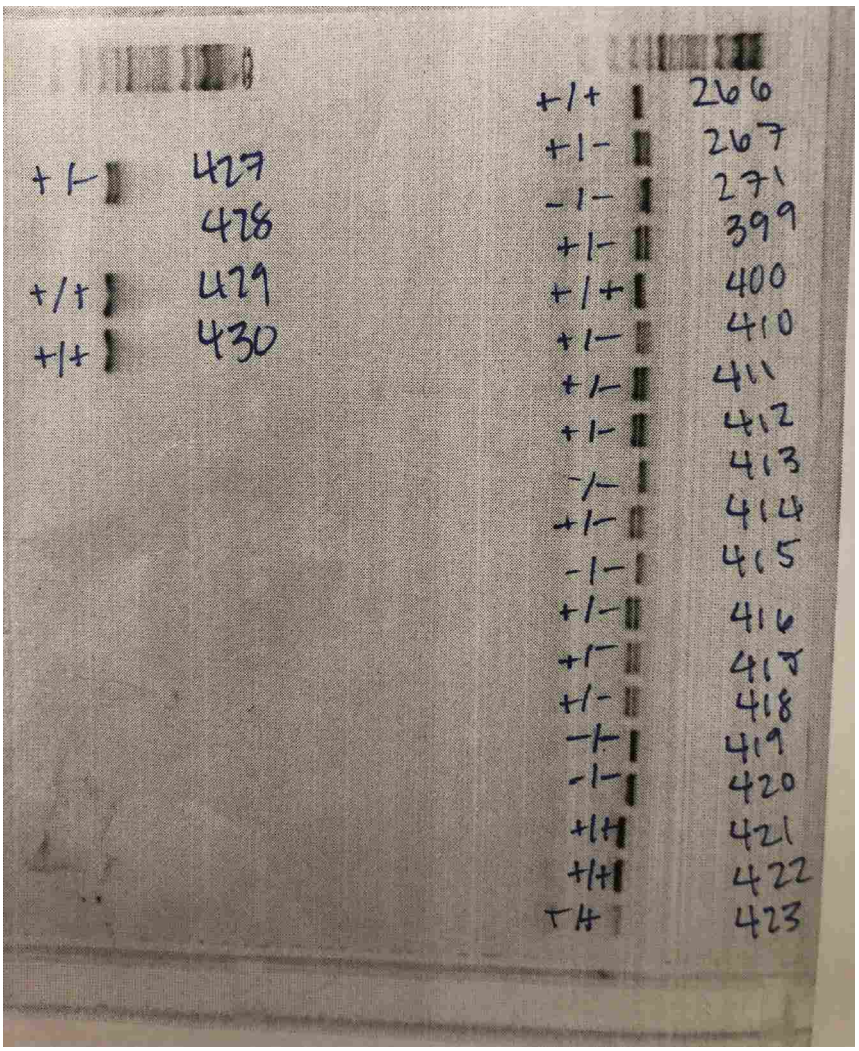

Figure 3. Representative image of genotyping results.

Insulin tolerance (ITT) and glucose tolerance testing (GTT) : All mice were fasted 6 hours prior to both GTT and ITT, with water freely available. Blood glucose levels were measured using the TRUEresult glucometer (Nipro diagnostics, Fort Lauderdale, FL). GTT was administered every four weeks at 3, 7, 11, 15, 19, and 23 weeks after weaning (Figure 4). A 20% glucose solution in PBS was injected intraperitoneally (IP) at a dose of 1mg/g body weight. An initial blood glucose reading was taken before injection with glucose. Blood glucose samples were measured at 5, 15, 30, 60, 90 and 120 minutes after injection. ITT was administered every four weeks at 16, 20 and 24 weeks after weaning (Figure 4). An initial blood glucose sample was measured, then 0.375 units/kg body weight of 0.5 U/ml insulin was administered IP (Humulin R; Lilly, Indianapolis,

IN). Blood glucose levels were measured at 15, 30, 45, 60, 90, and 120 minutes after injection. Mice with multiple readings below 20 mg/dL and demonstrating signs of insulin shock were IP injected with 100 ul of glucose and removed from the analysis. Food was made readily available and the mice were observed for recovery.

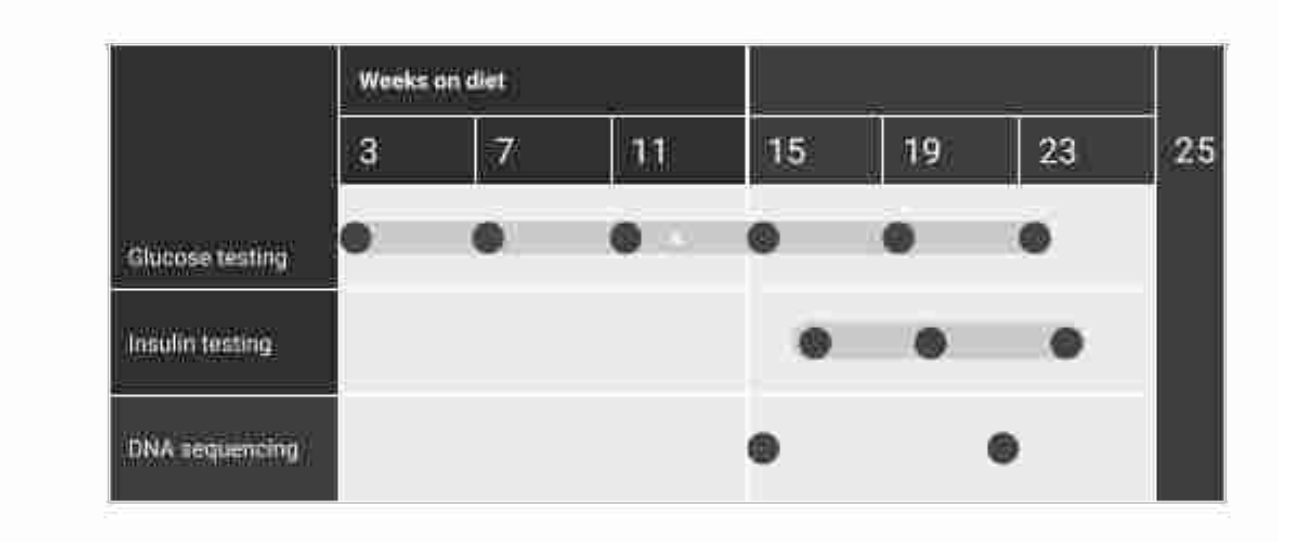

Figure 4. Outline of experimental plan. Dots indicate time points of experimental data collection.

Blood collection and tissue harvest: At 25 weeks of age mice were euthanized by cervical dislocation. Fresh blood was collected into a sterile Eppendorf tube. After 30 minutes blood samples were spun at 3000 rcf for 15 minutes at 4°C. The serum was collected and placed into a sterile tube and stored at -80°C. Excised tissues were immediately placed into sterile tubes with the following exceptions. The brain and pancreas were flash frozen on dry ice and then placed into sterile tubes. The left gonadal and retroperitoneal fat pads were weighed and then placed into sterile tubes. The liver was weighed, and the largest lobe was then divided into three sections. The first section was placed into 4% paraformaldehyde. The remaining two sections were placed into sterile tubes. The intestines were flushed with chilled PBS and then placed into sterile tubes. Contents of the cecum were removed and stored in a sterile tube. All samples were

then flash frozen in liquid nitrogen and stored at -80°C. Tissues not needed for this study have been saved for subsequent work.

Metagenomic analysis of gut microbiota

Bacterial DNA extraction, isolation, and purification protocol: Bacterial DNA was isolated and purified from fecal pellets stored at -80°C using the extraction protocol described in Godo [54] with the following changes: samples were homogenized in the Next Advance Bullet Blender Storm (Next Advance, Averill Park, NY), using 3.2 mm stainless steel beads (SSB32; Next Advance, Averill Park, NY). Cells were then disrupted with 0.1 mm glass beads (GB01; Next Advance, Averill Park, NY). After isolation, purified DNA was suspended in 10mM Tris (pH 8.5) and stored at -20°C.

Purity and concentration checks: DNA concentration was measured by absorbance at 260 nm (A260) and purity was estimated by measuring the A260/A280 ratio with a Nanodrop spectrophotometer (Nanodrop Technologies, Wilmington DE) (Table 1). Integrity of purified DNA was checked using 0.8% agarose gel electrophoresis with ethidium bromide staining (Figure 5a).

Table 1. Representative results of DNA concentration.

Sample ID	ng/ul	A260	A280	260/280	260/230	Constant	Cursor Pos.	Cursor abs.	340 raw
21-4	83.99	1.680	0.878	1.91	1.47	50.00	230	1.144	0.021
12-6	17.07	0.341	0.230	1.49	0.48	50.00	230	0.713	0.230
21-7	33.22	0.664	0.360	1.84	1.04	50.00	230	0.638	0.080
22-1	24.72	0.494	0.279	1.77	1.17	50.00	230	0.424	0.040
23-1	15.97	0.319	0.184	1.73	0.94	50.00	230	0.340	0.058
23-3	34.72	0.694	0.380	1.83	0.83	50.00	230	0.836	0.127
25-2	77.81	1.556	0.849	1.83	1.26	50.00	230	1.239	0.126
25-3	78.03	1.561	0.853	1.83	1.30	50.00	230	1.202	0.092
25-6	28.93	0.579	0.328	1.76	0.70	50.00	230	0.832	0.023
28-7	77.36	1.547	0.926	1.67	0.70	50.00	230	2.198	0.062
31-5	77.83	1.557	0.892	1.74	1.04	50.00	230	1.499	0.546
31-7	146.04	2.921	1.566	1.87	1.28	50.00	230	2.290	2.524
38-5	83.91	1.678	0.977	1.72	0.98	50.00	230	1.713	1.161
32-7	31.69	0.634	0.334	1.90	1.05	50.00	230	0.601	0.178
33-7	52.25	1.045	0.585	1.79	0.84	50.00	230	1.251	0.223

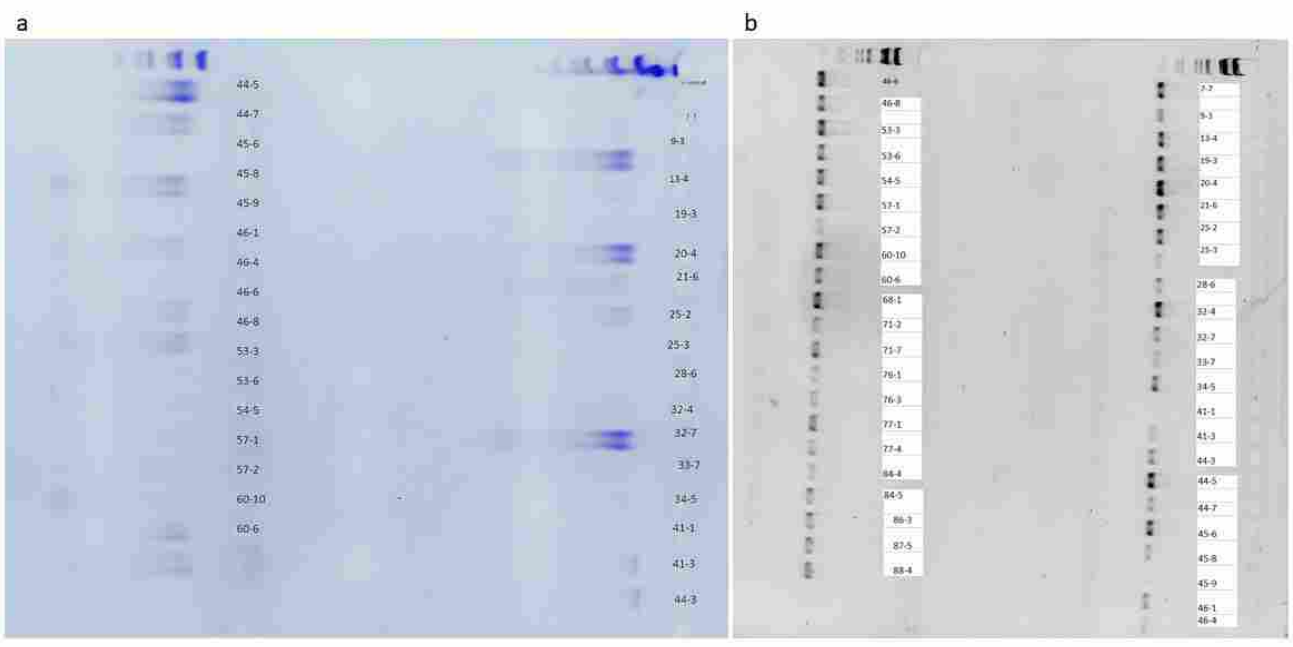

Figure 5. Representative gels from fecal DNA isolation and library preparation. (a) Bacterial genomic DNA from female week 22 samples. (b) Results from amplicon PCR, week 22 samples.

Bacterial DNA library preparation and sequencing: 16S rDNA gene libraries were prepared using the Mi-Seq protocol by Illumina with the following changes: Amplicon primer sequences provided by the Liping Zhao lab, Shanghai Jiao Tong University, were used to amplify the V3/V4 region of the 16S rDNA (Table 2), and integrity of PCR product was checked on 1.2% agarose gels (Figure 5b). Ampure beads were used for PCR cleanup. Illumina Nextera XT v2 adapters (Table 3) were then added using the Illumina protocol. Following index PCR, SequalPrep normalization plates (Invitrogen, Frederick, MD) were used for final DNA normalization of all samples**.** For the first batch of gut microbiota sequencing on male week 22 mice, samples were normalized manually by determining the concentration of DNA by Nanodrop then adjusting it appropriately (Table 4). Paired-end sequencing was performed on the Illumina Hi-Seq 2500 platform in the BYU DNA Sequencing Center.

Table 2. Primer sequences for 16s amplification.

Forward	PFV3V4	TCGTCGGCAGCGTCAGATGTGTATAAGAGACAGCCTACGGGNGGCWGCAG
	PFV3V4-1	TCGTCGGCAGCGTCAGATGTGTATAAGAGACAGTCCTACGGGNGGCWGCAG
	PFV3V4-2	TCGTCGGCAGCGTCAGATGTGTATAAGAGACAGCTCCTACGGGNGGCWGCAG
	PFV3V4-3	TCGTCGGCAGCGTCAGATGTGTATAAGAGACAGACTCCTACGGGNGGCWGCAG
	PFV3V4-4	TCGTCGGCAGCGTCAGATGTGTATAAGAGACAGGACTCCTACGGGNGGCWGCAG
	PFV3V4-5	TCGTCGGCAGCGTCAGATGTGTATAAGAGACAGAGACTCCTACGGGNGGCWGCAG
Reverse	PRV3V4	GTCTCGTGGGCTCGGAGATGTGTATAAGAGACAGGACTACHVGGGTATCTAATCC
	PRV3V4-1	GTCTCGTGGGCTCGGAGATGTGTATAAGAGACAGGGACTACHVGGGTATCTAATCC
	PRV3V4-2	GTCTCGTGGGCTCGGAGATGTGTATAAGAGACAGTGGACTACHVGGGTATCTAATCC
	PRV3V4-3	GTCTCGTGGGCTCGGAGATGTGTATAAGAGACAGATGGACTACHVGGGTATCTAATCC
	PRV3V4-4	GTCTCGTGGGCTCGGAGATGTGTATAAGAGACAGCATGGACTACHVGGGTATCTAATCC
	PRV3V4-5	GTCTCGTGGGCTCGGAGATGTGTATAAGAGACAGACATGGACTACHVGGGTATCTAATCC

Table 3. Plate layout and list of Illumina indexing adapters used in the sequencing library.

Nextera XT v2 Set	Primer set 1	Primer set 2
A	N701-N715	S502-S511
B	N716-N729	S502-S511
C	N701-N715	S513-S522

Table 4. Representative results of DNA concentration after PCR-based incorporation of Illumina adapters and clean-up.

Sample ID	ng/ul	A260	A280	260/280	260/230	Constant	Cursor Pos.	Cursor abs.	340 raw
A1	21.10	0.422	0.235	1.80	2.90	50.00	230	0.146	0.440
A2	43.10	0.862	0.640	1.35	0.93	50.00	230	0.925	6.055
A3	7.10	0.142	0.123	1.15	3.88	50.00	230	0.037	0.436
A4	26.83	0.537	0.316	1.70	2.65	50.00	230	0.202	0.456
A5	17.62	0.352	0.210	1.68	2.49	50.00	230	0.142	0.445
A6	18.27	0.365	0.222	1.65	2.91	50.00	230	0.126	0.465
A7	10.96	0.219	0.160	1.37	4.55	50.00	230	0.048	0.437
A8	13.77	0.275	0.167	1.65	3.60	50.00	230	0.076	0.480
A10	8.60	0.172	0.127	1.35	3.37	50.00	230	0.051	0.453
A11	11.75	0.235	0.151	1.56	3.17	50.00	230	0.074	0.457
A12	27.79	0.556	0.331	1.68	2.82	50.00	230	0.197	0.457
B1	18.35	0.367	0.257	1.43	2.59	50.00	230	0.142	0.069
B1	17.36	0.347	0.193	1.80	3.32	50.00	230	0.105	0.444

Sequencing analysis: 16S rDNA sequences were analyzed using the QIIME2/2017.10. software package [55]. Read joining, denoising, demultiplexing, and feature assignments were accomplished using the Dada2 [56] plug-in. Forward reads were truncated 23 bp to trim amplicon primers. Reverse reads were truncated at 249 and 240 base pairs to insure overlap of reads. Samples from the created BIOM table [57] were then filtered to remove features that appear in less than 2 total samples (singletons), samples that contain less than 10 features and features not assigned to at least phyla level. Phylogenetic distances were computed using q2-feature-classifier [58] with naïve-bayes fit [59]. Alpha and beta diversity were calculated using core metrics rarefied to a sampling

depth of 8000. Principle coordinate analysis (PCoA) visualizations were created using EMPeror [60,61]. Permutation Multivariate Analysis of Variance (PERMANOVA) [62] was used to compare differences in beta diversity between groups. Alpha diversity was calculated using Faith's Phylogenetic Diversity (PD) and Kruskal-Wallis one-way analysis of variance [63,64]. Taxonomy was assigned using q2-feature-classifier plug-in [65] using Greengenes13_8 85% OTUs trained with the following primer sequences: F-CCTACGGGNGGCWGCAG R-GACTACHVGGGTATCTAATCC.

Immunoblotting

Homogenization : Colon and skeletal muscle samples were weighed and lysed in 2X RIPA buffer volume/sample volume, with 10 µl/ml protease and phosphatase inhibitor cocktail (#78440, Thermo Fisher, Rockford, IL). All samples were homogenized using the Bullet Blender Storm 24 (Next Advance, Averill Park, NY). Samples were homogenized using 0.9-2 mm stainless steel beads. Muscle samples were homogenized at speed 10 for 4 minutes and colon samples were homogenized at speed 12 for 3 minutes. Following homogenization and lysis, samples were centrifuged at 16,000 rcf for 10 minutes and the supernatant was collected and stored at -80°C.

Protein assay : Protein levels were quantified using the Pierce BCA Assay Kit (Thermo Fisher, Rockford, IL) and a microplate reader (BioTek , Minooski, VT). Due to high protein concentration, colon and muscle samples were diluted 1:10 and 1:100 respectively for accuracy in detection. A linear equation was extrapolated using protein standards and associated optical density readings (Figure 6), and protein concentration of unknown samples was estimated using that equation (Table 5).

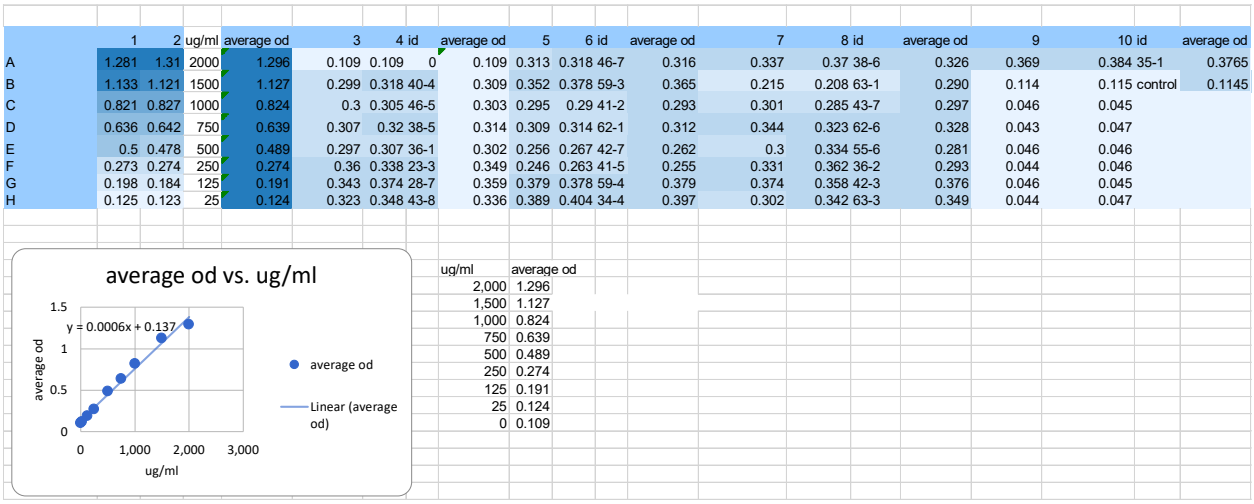

	1	2	ug/ml	average od	3	4	id	average od	5	6	id	average od	7	8	id	average od	9	10	id	average od
A	1.281	1.31	2000	1.296	0.109	0.109	0	0.109	0.313	0.318	46-7	0.316	0.337	0.37	38-6	0.326	0.369	0.384	35-1	0.3765
B	1.133	1.121	1500	1.127	0.299	0.318	40-4	0.309	0.352	0.378	59-3	0.365	0.215	0.208	63-1	0.290	0.114	0.115	control	0.1145
C	0.821	0.827	1000	0.824	0.3	0.305	46-5	0.303	0.295	0.29	41-2	0.293	0.301	0.285	43-7	0.297	0.046	0.045		
D	0.636	0.642	750	0.639	0.307	0.32	38-5	0.314	0.309	0.314	62-1	0.312	0.344	0.323	62-6	0.328	0.043	0.047		
E	0.5	0.478	500	0.489	0.297	0.307	36-1	0.302	0.256	0.267	42-7	0.262	0.3	0.334	55-6	0.281	0.046	0.046		
F	0.273	0.274	250	0.274	0.36	0.338	23-3	0.349	0.246	0.263	41-5	0.255	0.331	0.362	36-2	0.293	0.044	0.046		
G	0.198	0.184	125	0.191	0.343	0.374	28-7	0.359	0.379	0.378	59-4	0.379	0.374	0.358	42-3	0.376	0.046	0.045		
H	0.125	0.123	25	0.124	0.323	0.348	43-8	0.336	0.389	0.404	34-4	0.397	0.302	0.342	63-3	0.349	0.044	0.047		

ug/ml	average od
2,000	1.296
1,500	1.127
1,000	0.824
750	0.639
500	0.489
250	0.274
125	0.191
25	0.124
0	0.109

Figure 6. Representative results from protein quantification. 1:100 serial dilution of muscle lysates.

Table 5. Representative results of protein concentration.

id	average od	protein ug/ml
46-7	0.3155	28605.77
59-3	0.365	36538.46
41-2	0.2925	24919.87
62-1	0.3115	27964.74
42-7	0.2615	19951.92
41-5	0.2545	18830.13
59-4	0.3785	38701.92
34-4	0.3965	41586.54
40-4	0.3085	27483.97

Protein sample preparation : Equal amounts of protein from colon lysates (Table 6) were combined with 5X Lane Marker Sample Buffer (Thermo Fisher, Rockford, IL), heated in a boiling water bath for 5 minutes, and then loaded onto a 4-15% SDS-PAGE gradient mini-PROTEAN TGX gel,15 µl/well volume (Bio-Rad, Hercules, CA) for separation. Muscle samples were treated with 2X Laemmli Sample Buffer (Bio-Rad, Hercules, CA), heated for 5 minutes in boing water and loaded onto an Any kD mini-PROTEAN TGX gel, 20 µl/well volume.

Table 6. Representative table of loading volumes of muscle lysates for immunoblotting.

ID	average od	protein amt(x100)	protein vol (30 ug)	ripa vol (5 ul total)	sample loading buffer vol	total vol
46-7	0.3155	28605.77	1.05	3.95	5	10
59-3	0.365	36538.46	0.82	4.18	5	10
41-2	0.2925	24919.87	1.20	3.80	5	10
62-1	0.3115	27964.74	1.07	3.93	5	10
42-7	0.2615	19951.92	1.50	3.50	5	10
41-5	0.2545	18830.13	1.59	3.41	5	10
59-4	0.3785	38701.92	0.78	4.22	5	10
34-4	0.3965	41586.54	0.72	4.28	5	10
40-4	0.3085	27483.97	1.09	3.91	5	10
46-5	0.3025	26522.44	1.13	3.87	5	10
38-5	0.3135	28285.26	1.06	3.94	5	10
36-1	0.302	26442.31	1.13	3.87	5	10
23-3	0.349	33974.36	0.88	4.12	5	10
28-7	0.3585	35496.79	0.85	4.15	5	10
43-8	0.3355	31810.90	0.94	4.06	5	10

Immunoblotting : An internal standard (WT-NCD) was included on every gel for normalization comparison between gels. Semi-dry electrotransfer of proteins to a 0.45µm nitrocellulose membrane in transfer buffer (20% methanol in tris/glycine buffer) was performed using the Bio-Rad Trans-Blot Turbo (Invitrogen, Carlsbad, CA) mixed MW midi program. After transfer to the nitrocellulose membrane, non-specific proteins were blocked in a 5% milk solution (7.5 g non-fat dry milk, 150 ml 1X tris-buffered saline (TBS)) and washed in TBST, 0.5ml Tween-20 in 1L TBS. The membrane was then incubated overnight with primary antibodies at 1:1000 dilution (TNF-α, claudin-1, β-Actin, GAPDH, Akt, pAkt(Ser473) Cell Signaling, Danvers, MA), diluted in BSA (2.5g bovine serum albumin in 50 ml TBST). Muscle samples were probed for GAPDH as a loading control. β-Actin was used as a loading control in liver and colon samples. Following overnight incubation and washing, the membrane was then incubated for 60 minutes under foil

with secondary antibodies, 1:10,000 dilution (IRDye 680RD goat/anti-rabbit, IRDye 800CW donkey/anti-mouse LI-COR, Lincoln, NE) in BSA and washed with TBST.

Imaging and quantification : Membranes were imaged (Figure 7) on the LI-COR reader using default parameters. Protein expression levels were evaluated and using the LI-COR imaging software. The resulting readings were then normalized against the WT-NCD control. β-actin levels were used as a loading control, and any samples with β-actin <0.7 or >1.3 relative to the control lanes were discarded (Table 7).

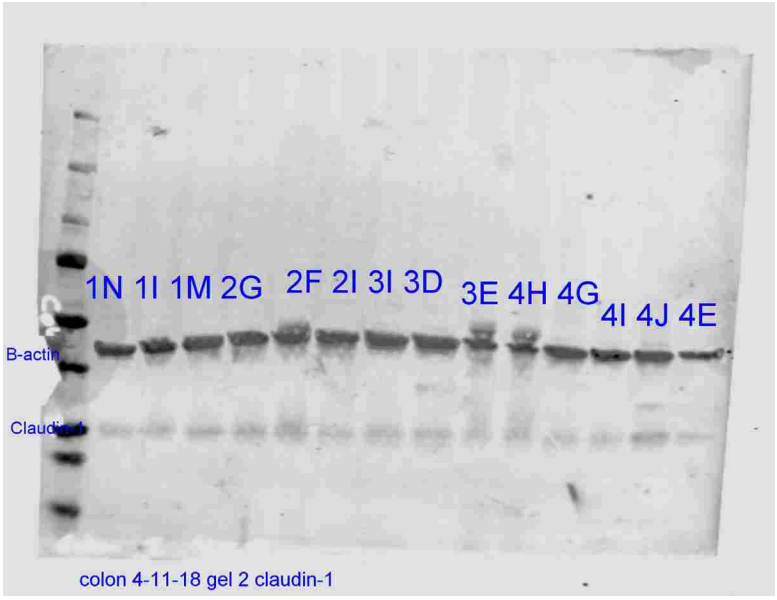

Figure 7. Representative image of Western Blot.

Table 7. Representative normalization and quantification of western blot band densities from Figure 7. Highlighted values (upper Claudin-1, ex. 2.15Claudin-1) values were discarded from analysis due to low relative control (lower β-actin, ex 2.15B-actin) values.

Image Name	Name	Signal	Area	2.2 B-actin		
0002559_03	2.2 Claudin-1	1637.694336	319	1.000	0.037	1N
0002559_03	2.3 Claudin-1	1350.521484	319	0.825	0.031	1I
0002559_03	2.4 Claudin-1	2208.875	319	1.349	0.055	1M
0002559_03	2.5 Claudin-1	2043.830078	319	1.248	0.055	2G
0002559_03	2.6 Claudin-1	2088.988281	319	1.276	0.065	2F
0002559_03	2.7 Claudin-1	881.9785156	319	0.539	0.025	2I
0002559_03	2.8 Claudin-1	1343.277344	319	0.820	0.033	3I
0002559_03	2.9 Claudin-1	1574.375	319	0.961	0.038	3D
0002559_03	2.1 Claudin-1	937.8847656	319	0.573	0.033	3E
0002559_03	2.11 Claudin-1	1276.253906	319	0.779	0.048	4H
0002559_03	2.12 Claudin-1	931.5380859	319	0.569	0.025	4G
0002559_03	2.13 Claudin-1	857.3457031	319	0.524	0.022	4I
0002559_03	2.14 Claudin-1	2731.742188	319	1.668	0.084	4J
0002559_03	2.15 Claudin-1	1023.404297	319	0.625	0.040	4E

				2.2
0002559_03	2.2 B-actin	43986.51953	420	1.000
0002559_03	2.3 B-actin	43106.80469	420	0.980
0002559_03	2.4 B-actin	40438.51563	420	0.919
0002559_03	2.5 B-actin	37351.65234	420	0.849
0002559_03	2.6 B-actin	32374.30859	420	0.736
0002559_03	2.7 B-actin	34694.44141	420	0.789
0002559_03	2.8 B-actin	41027.27539	420	0.933
0002559_03	2.9 B-actin	41783.05078	420	0.950
0002559_03	2.1 B-actin	28180.22656	420	0.641
0002559_03	2.11 B-actin	26656.83984	420	0.606
0002559_03	2.12 B-actin	37023.84766	420	0.842
0002559_03	2.13 B-actin	38537.7793	420	0.876
0002559_03	2.14 B-actin	32482.09375	420	0.738
0002559_03	2.15 B-actin	25453.87891	420	0.579

Statistical Analysis

All data are shown as mean ± SEM using GraphPad Prism 7.0. Multiple groups were analyzed using ANOVA with Sidak's or Tukey's multiple comparisons test in GraphPad Prism. Alpha diversity of microbiota data was analyzed using Kruskal-Wallis one-way ANOVA [63]. Permutation Multivariate Analysis of Variance (PERMANOVA) [62] was used to compare differences in beta diversity between groups. Area under the curve was calculated with a baseline of 0. Significance levels were assigned as $p<0.05$; *$p<0.05$, **$p<0.01$, ***$p<0.001$, ****$p<0.0001$. Tertiles were assigned by sorting each group sequentially and dividing the rankings into thirds.

Results

PASK deletion does not protect against weight gain on a HFHS diet.

The aim of this research was to determine whether PASK-deficient mice would be protected from weight gain and insulin resistance when placed on a Western diet--one high in both fats and sugars, as when fed a high-fat only diet [47,49]. Significant increases in weekly weight gain were seen in both $PASK^{+/+}$ (WT-HFHS) and $PASK^{-/-}$ (MUT-HFHS) (Figures 8a and 8b) male mice on the HFHS diet over time. Additionally, both WT-HFHS ($p=0.0010$) and MUT-HFHS ($p=0.0246$) had significantly higher final body weights when compared to NCD (Figure 8c). However, no significant differences in weight gain or final weights were seen between the genotype groups on either diet. Likewise, relative weights of whole liver (WT $p=2.472e-009$, MUT $p=1.218e-007$), as well as gonadal (GFP) (WT $p=0.0511$, MUT $p=0.01091$) and retroperitoneal fat pads (RFP) (WT $p=0.0021$, MUT $p=2.47e-005$) showed differences reflective of diet, not genotype (Figures 8d, 8e, and 8f).

Results of weight gain in the female mice showed that the MUT-HFHS mice gained more weight overall than all other groups (Figure 8h), with significant differences in final weights between MUT-HFHS and WT-HFHS ($p=.00024$) and MUT-NCD ($p=0.0002$) (Figure 8i). Unfortunately, female WT-HFHS mice failed to gain more weight than wild type females on the normal chow diet (WT-NCD) (Figure 8g). All female mice were subsequently dropped from the analysis due to failure to validate the method of inducing weight gain through HFHS diet in the control group.

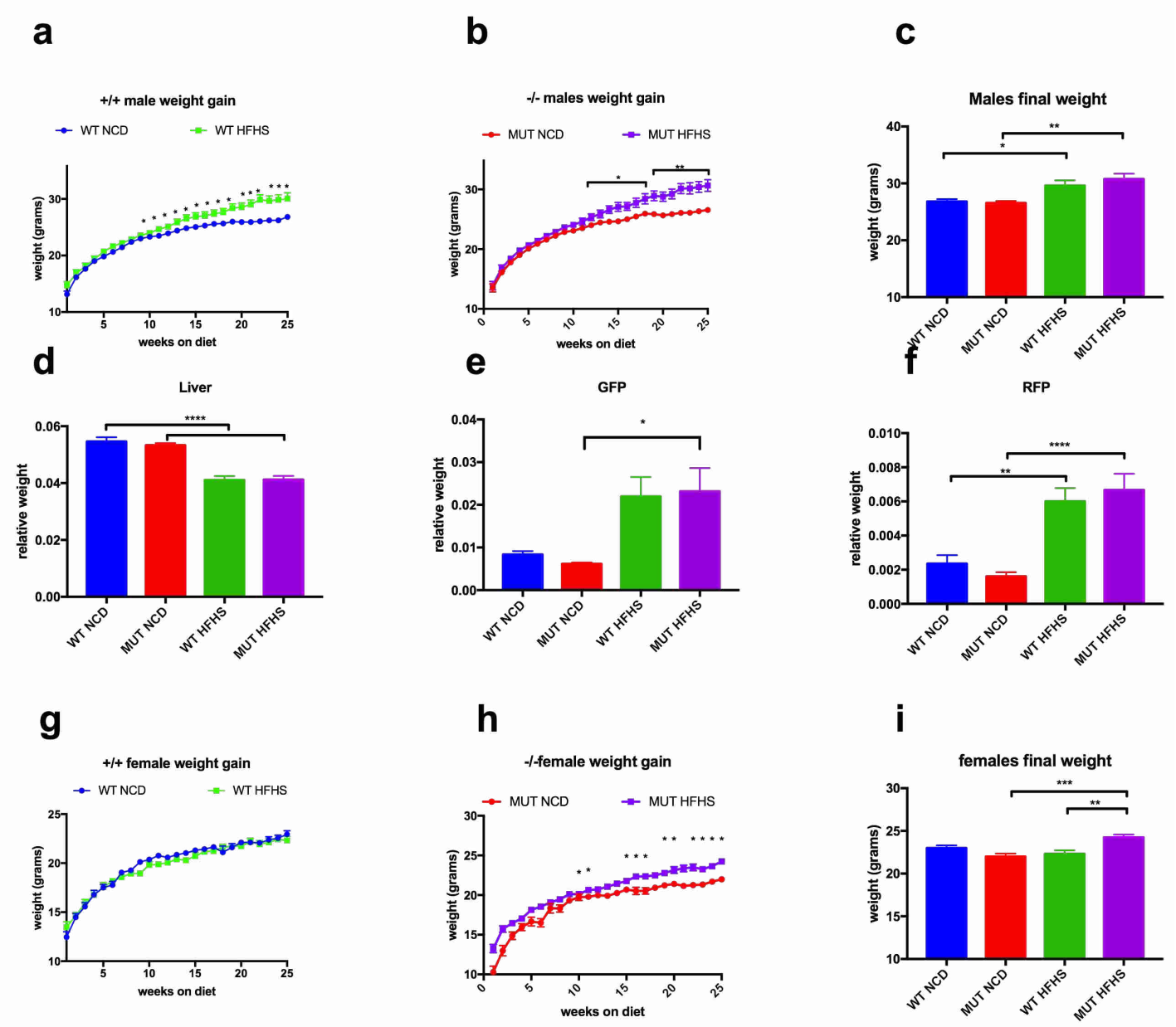

Figure 8. Diet, not genotype, influences body and tissue weight. (a) Weekly body weight gain of WT male mice by diet. Significant differences emerged after 11 weeks on the diet ($p<0.05$). (b) Weekly body weight gain of MUT male mice by diet. (c) Male final body weights. (d-f) Relative tissue weights at dissection of liver, gonadal fat pad, and retroperitoneal fat pad expressed as tissue weight/final body weight. (g, h) Female weight gain by week. (i) Female final weights. All data is expressed as mean ± SE. All groups n=13-19.

PASK deletion does not significantly alter blood glucose levels.

Previous research has shown deletion of PASK imparts a protective effect against high-fat diet-induced insulin resistance [47,53]. Our research showed no significant differences in fasting blood glucose levels between the groups (Figure 9a). Additionally, no significant differences were seen in glucose response or area under the curve between all mice in the groups at mid-testing, 15 weeks (Figures 9b and 9c), 19 weeks (Figures 9d and 9e) or the final time point, 23 weeks (Figures 9f and 9g). There was a trend seen with ITT response at 16 weeks between MUT-NCD and MUT-HFHS mice (Figures 10a and 10b), but any differences failed to repeat in subsequent tests (Figures 10c and 10d).

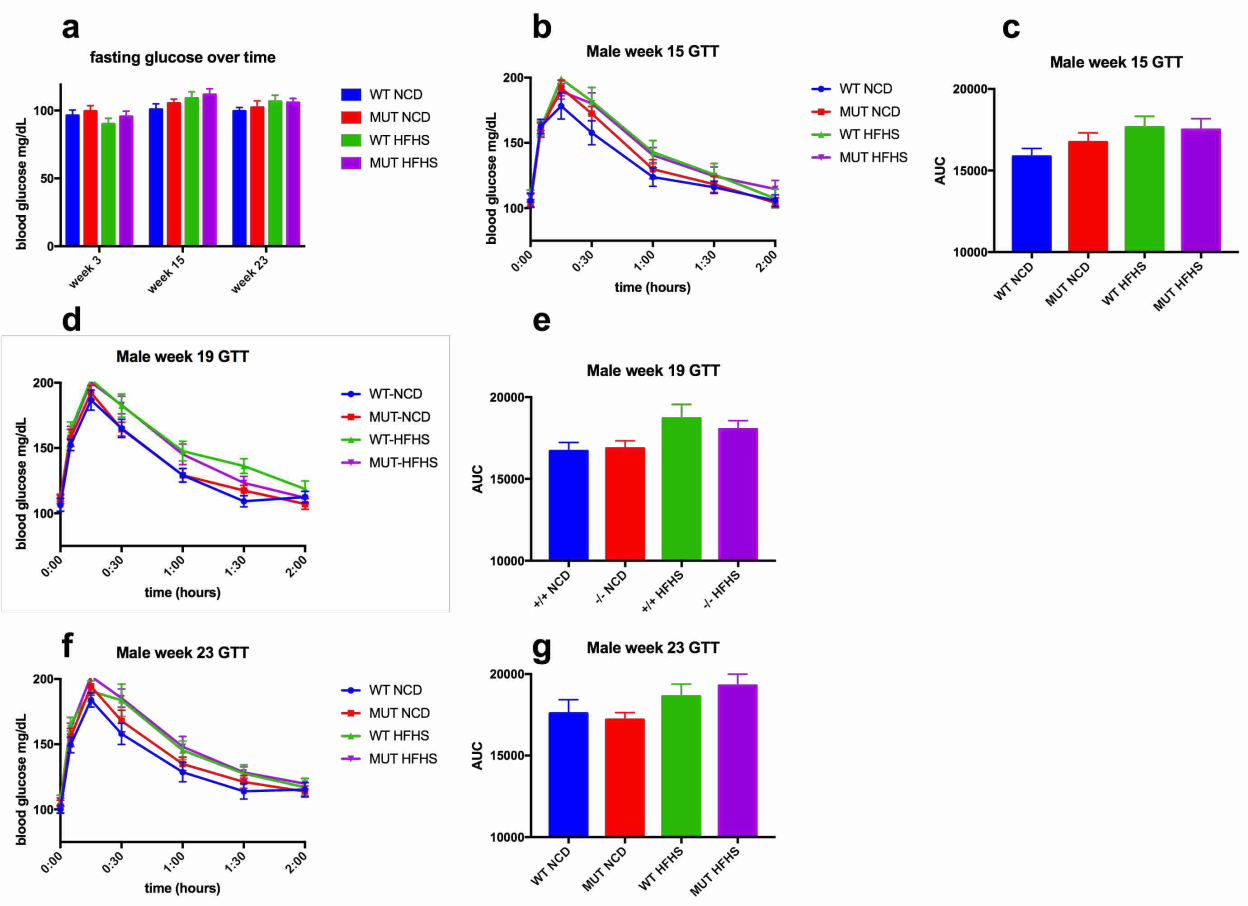

Figure 9. WT and MUT mice show no difference in glucose tolerance. (a) Fasting blood glucose levels after 3, 15, and 23 weeks on diet. (b-e) Blood glucose levels during IP gluocose tolerance testing and area under the curve. All groups n=12-15.

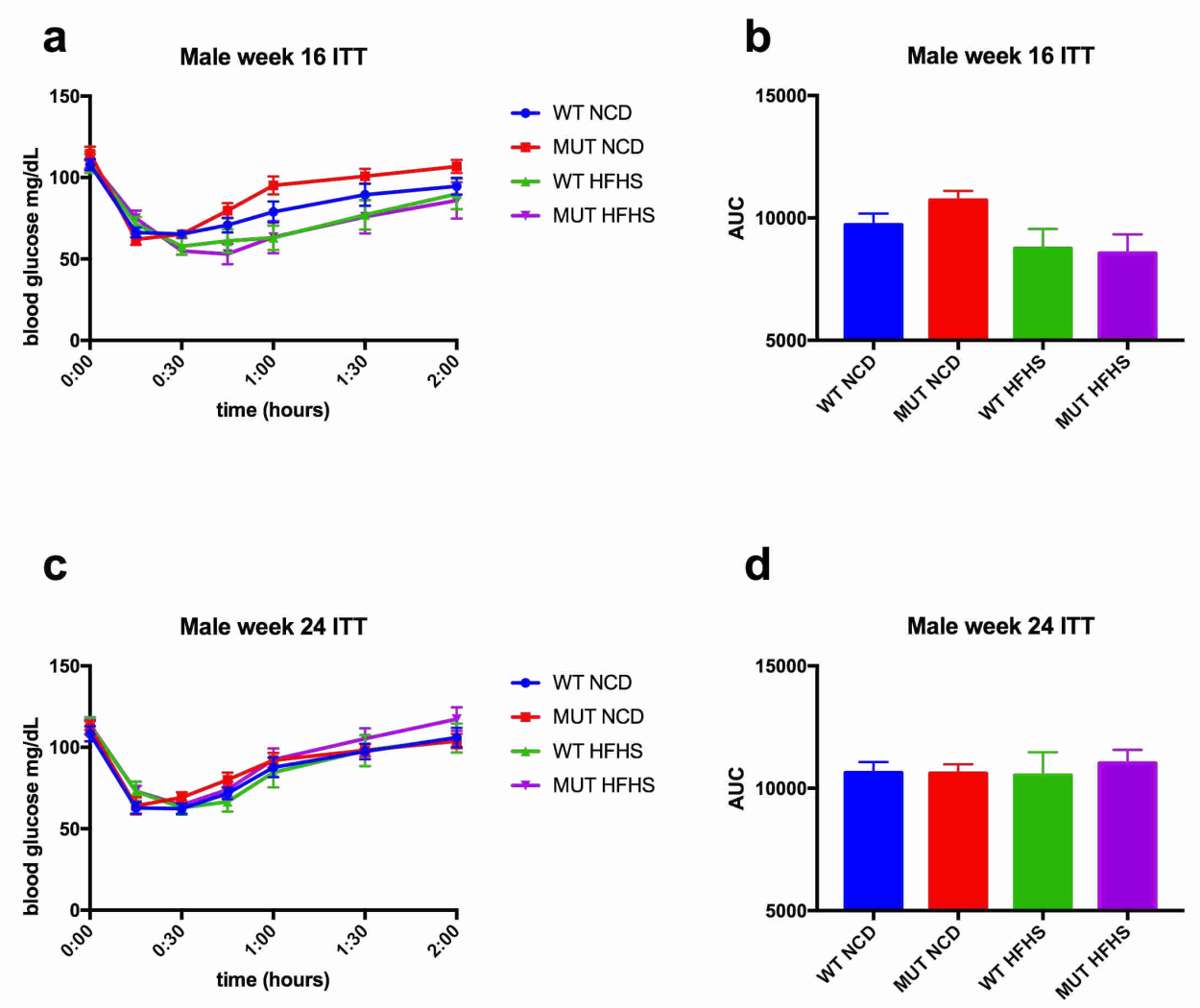

Figure 10. Insulin tolerance testing showed no differences between groups. (a) week 16 (b) week 16 AUC (c) week 24 (d) week 24 AUC. All groups n=12-15

Claudin-1 expression is dependent on diet.

To better understand the increased weight gain and insulin resistance seen in the MUT-HFHS mice, protein levels of claudin-1 in the colon, and Akt and pAkt in skeletal muscle were measured by immunoblotting. Claudin-1 is a membrane protein involved in forming the tight junctions between intestinal endothelial cells. Claudin-1 levels have been shown to be reduced in mice on a high-fat diet [37]. Colon claudin-1 expression significantly decreased in WT-HFHS mice compared to WT-NCD mice (Figure 12a, p=0.0004). Surprisingly, MUT-HFHS mice showed increased claudin-1 expression when compared to WT-HFHS mice (Figure 11a, p=0.007).

Akt levels in the skeletal muscle show a decreasing trend in MUT-NCD when compared to WT-NCD mice (Figure 11b p=0.06). Akt expression levels were similar between all mice on the HFHS diet and WT-NCD mice. Relative levels of activated Akt (pAkt ser473) decreased in mutants, with significant decreases seen in the MUT-HFHS mice (Figure 11c, p=0.01) when compared to WT-HFHS, conflicting with the Claudin-1 results and previously published liver data from high-fat fed PASK knockout mice [48].

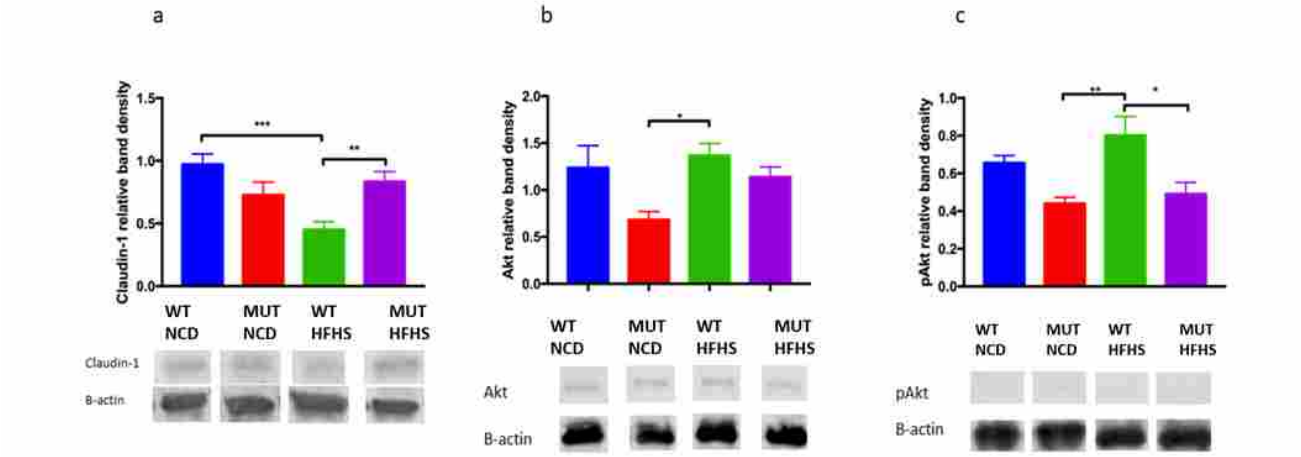

Figure 11. Diet and genotype induced changes in protein levels. (a) Colon claudin-1 levels. N=5-7 per group. (b) Muscle Akt levels. N=3-5 per group, (c) Muscle pAkt(ser473) levels. N=4-5 per group. Representative immunoblots are shown.

The gut microbiome reflects diet, not genotype

To study the effects of PASK and diet on the gut microbiota, fecal samples collected after 22 weeks on the diet were selected for bacterial DNA isolation and sequencing. This time point was chosen for maximum length of time on the diet, and longest amount of time after blood glucose testing (2 weeks) to minimize any effects of stress. Preliminary results of the unweighted Unifrac principle coordinate analysis (PCoA) plot showed a clear separation by diet with the NCD mice closely clustered together (Figure 12a, blue dots). Genotype did not influence

separation of the samples with both genotypes equally dispersed among diet groups (Figure 12b). Mutant samples on the HFHS diet showed a separation into two clusters, yellow and orange circles, (Figure 12d), with the differences in microbiota composition reflected in a poor response to glucose at 15 weeks in the upper/orange cluster, (Figure 12c). “Because the difference in glucose response was more pronounced at 15 weeks (Figure 12c) than at 22 weeks (not shown), another batch of 16S rDNA gut microbiota sequencing was performed using samples collected after 15 weeks on the diet. To minimize variability, 22-week samples were re-sequenced with the 15-week samples.

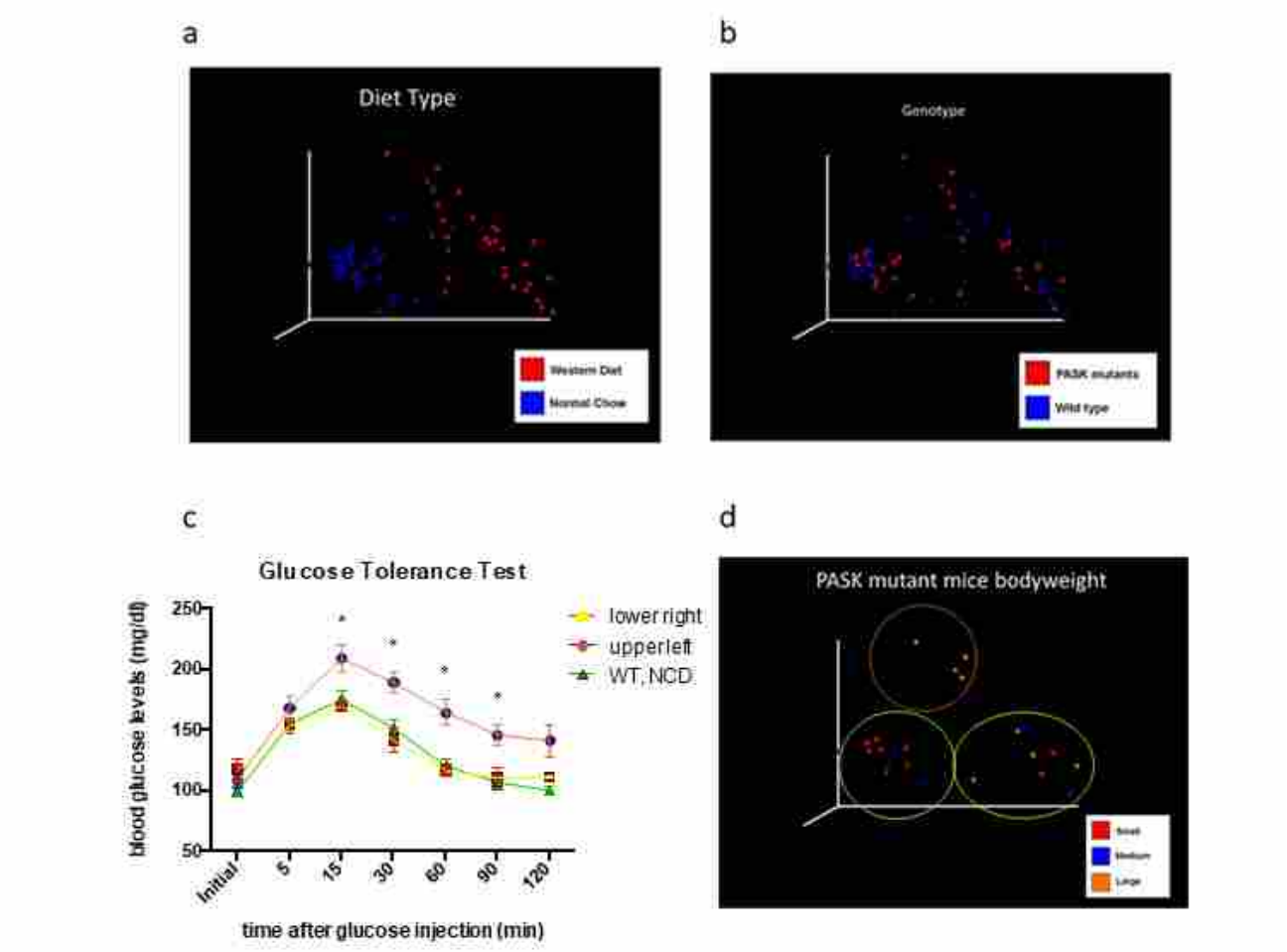

Figure 12. Microbial composition influenced glucose tolerance at 15 weeks. Unweighted Unifrac PCoA plots of male, week 22 samples coded by (a) diet (b) genotype (c) glucose tolerance results of MUT-HFHS males separated by cluster. (d) Unweighted UniFrac PCoA plot coded by body weight tertile

Gut microbiota composition is determined by diet, not genotype

When comparing genotype, samples taken after both 15 and 22 weeks on the diet showed no differences in alpha diversity (Faith's Phylogenetic Diversity) [64] (15-week HFHS n=12-13, p=0.586; NCD n=10-11, p=0.324. 22-week NCD n=13-16, p=0.93. HFHS n=12-15, p=0.96) (Figure 13a) or beta diversity (unweighted Unifrac)[66] (15-week NCD p= 0.314, HFHS p=0.672. 22-week NCD p=0.183, HFHS p=0.579) (Figure 13b). Diet however, played a significant role in shaping differences in alpha (15-week n=21-25, p=0.00002 H=18.2, q=0.0002. 22-week n=27-29, p=0.002 H=9.55) (Figure 13c) and beta diversity after both 15 and 22 weeks on the diet (15-week p= 0.001, 22-week p=0.001) (Figure 13d). Differences in diversity were reflected with increases in the relative abundance of Actinobacteria in mice on the HFHS diet after both 15 (Figure 13e) and 22 weeks on the diet (Figure 13f) and a decrease in the abundance of Bacteroidetes only after 22 weeks (Figure 13f). These results suggest that diet played the determinative role in the composition of the gut microbiota.

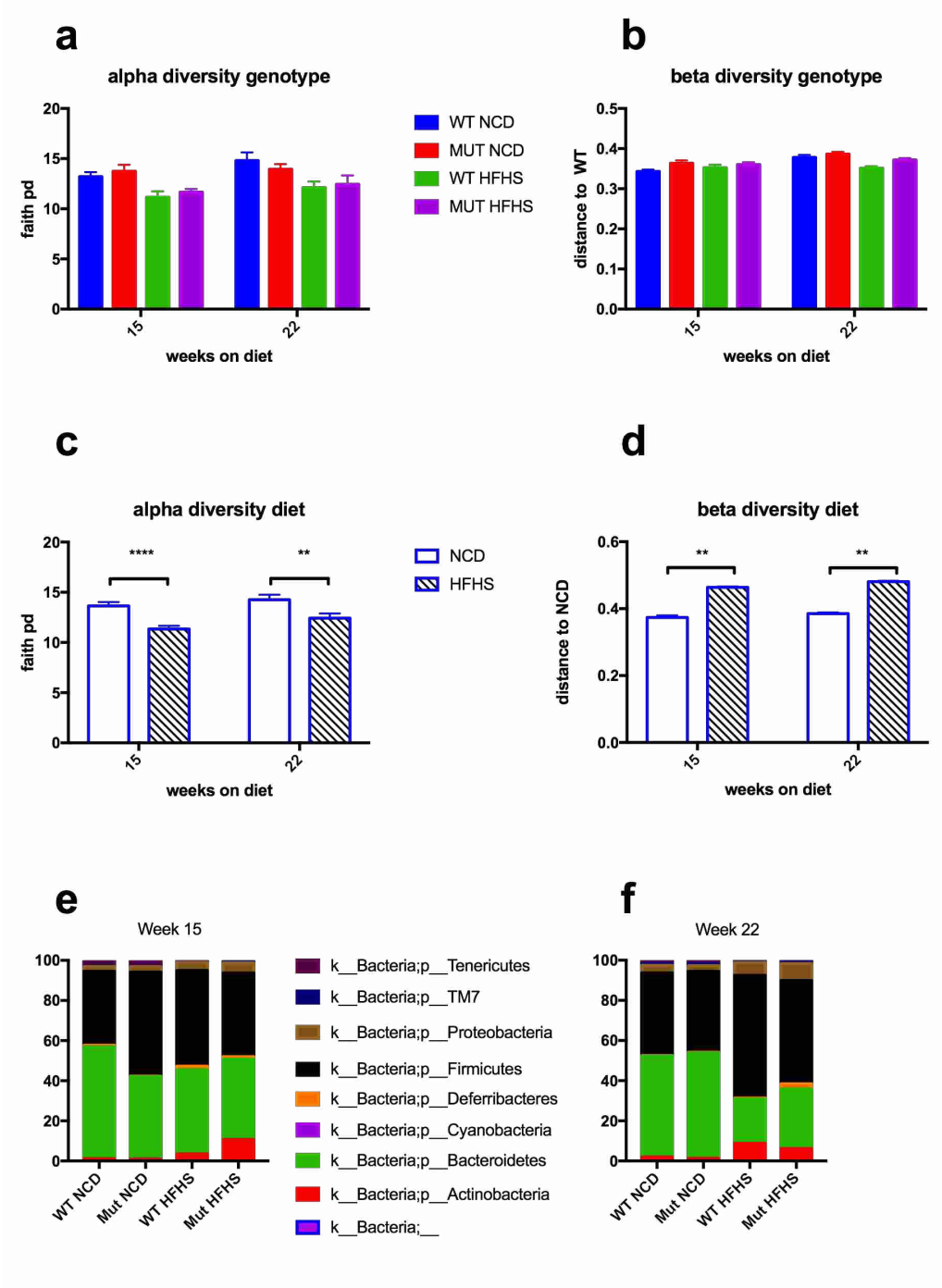

Figure 13. Diet, not genotype, influences gut microbial diversity. Alpha diversity is measured by Faith's Phylogenetic Diversity. Beta diversity is a measurement of. (a).Comparison of Faith's Phylogenetic Diversity between genotypes (b) Comparison of unweighted UniFrac distances by genotype (c) Comparison of Faith's Phylogenetic Diversity between NCD and HFHS (d) Comparison of unweighted UniFrac distances between NCD and HFHS. (e) Relative abundance at phyla level of week 15 samples. (f) Relative abundance at phyla level of week 22 samples. Alpha diversity is expressed as mean plus SEM, distances to NCD with Kruskal-Wallis follow-up. Beta diversity is expressed as mean plus SEM with PERMANOVA comparison.

Bacterial composition is associated with weight gain and glucose response in HFHS mice.

To further study the roles diet and microbiota composition played in the development of obesity and glucose intolerance, we analyzed Unweighted Unifrac Principle Coordinate Analysis (PCoA) results. After the second round of sequencing, week 15 PCoA results reflected separation only by diet (Figure 14a). Week 22 PCoA results showed the same separation of the HFHS mice into two distinct groups (Figure 14b) as was seen previously (Figure 12d). HFHS mice that fell into the upper third of final body weight per group (1^{st} tertile, triangles) were all in the lower (orange oval) cluster on the PCoA plot (Figure 14b). This cluster showed higher levels of *Firmicutes* and *Bacteroidetes* (Figure 14c) and is reflected in Unweighted Unifrac distances between the first tertile of final body weight and the second tertile in HFHS week 22 samples (Figure 14d) ($p=0.003$), but not in the 15-week samples, suggesting the microbiota shift in the HFHS developed over time. The HFHS lower cluster also had significantly higher final body weights (Figure 14e) when compared to the WT-NCD ($p=0.0478$), whereas the HFHS upper cluster did not ($p=0.1854$). These data suggest the microbiota shift that occurred in some mice on the HFHS diet was a factor in the development of obesity.

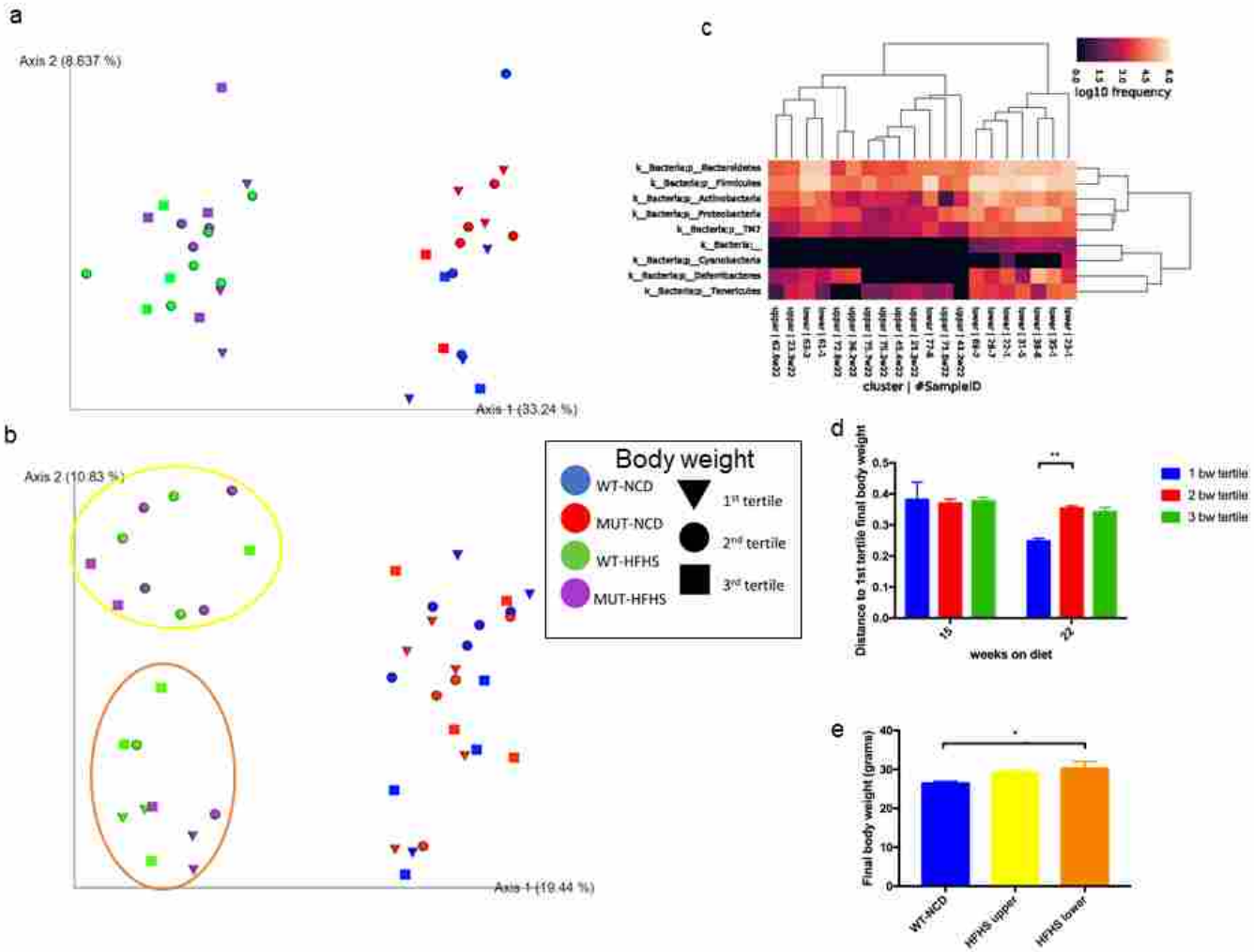

Figure 14. Gut microbial composotion influences weight gain. (a) Unweighted UniFrac PCoA plot of week 15 samples. (b) Unweighted UniFrac PCoA plot of week 22 samples coded by final body weight tertile per group, orange oval outlines the HFHS lower cluster, yellow oval outlines the HFHS upper cluster. (c) Heatmap of week 22 male HFHS samples sorted by final body weight tertile. (d) Comparison of unweighted UniFrac distances by final body weight tertile of HFHS males. (e) Final body weights of HFHS mice divided by unweighted UniFrac PCoA cluster.

Comparison of glucose responses between the two clusters revealed neither cluster was significantly different from WT-NCD at week 15 GTT (Figure 15a and Figure 15b, p= 0.0961) An impaired glucose response in the lower cluster was seen at week 19 GTT (Figure 15c and Figure 15d, p=0.0040), and week 23 GTT (Figure 15e and Figure 15f, p=0.0185) when compared to WT-NCD. When GTT results were divided into tertiles, mice whose week 19 GTT AUC results were in the top (worst) tertile for their group were all in the lower gut microbiota cluster (Figure 15g), and their gut microbiota showed a separation from the middle tertile reflected in unweighted UniFrac distances (Figure 15h) (p=0.015). Similar separation by GTT tertile were not seen at the 15-week timepoint (Figure 15h), again suggesting that the gut microbiotas shifted over time. ITT results were not correlated with microbiota composition (week 16 ITT AUC p=0.2916, Figure 15i; week 24 ITT AUC p=0.3839, Figure 15j).

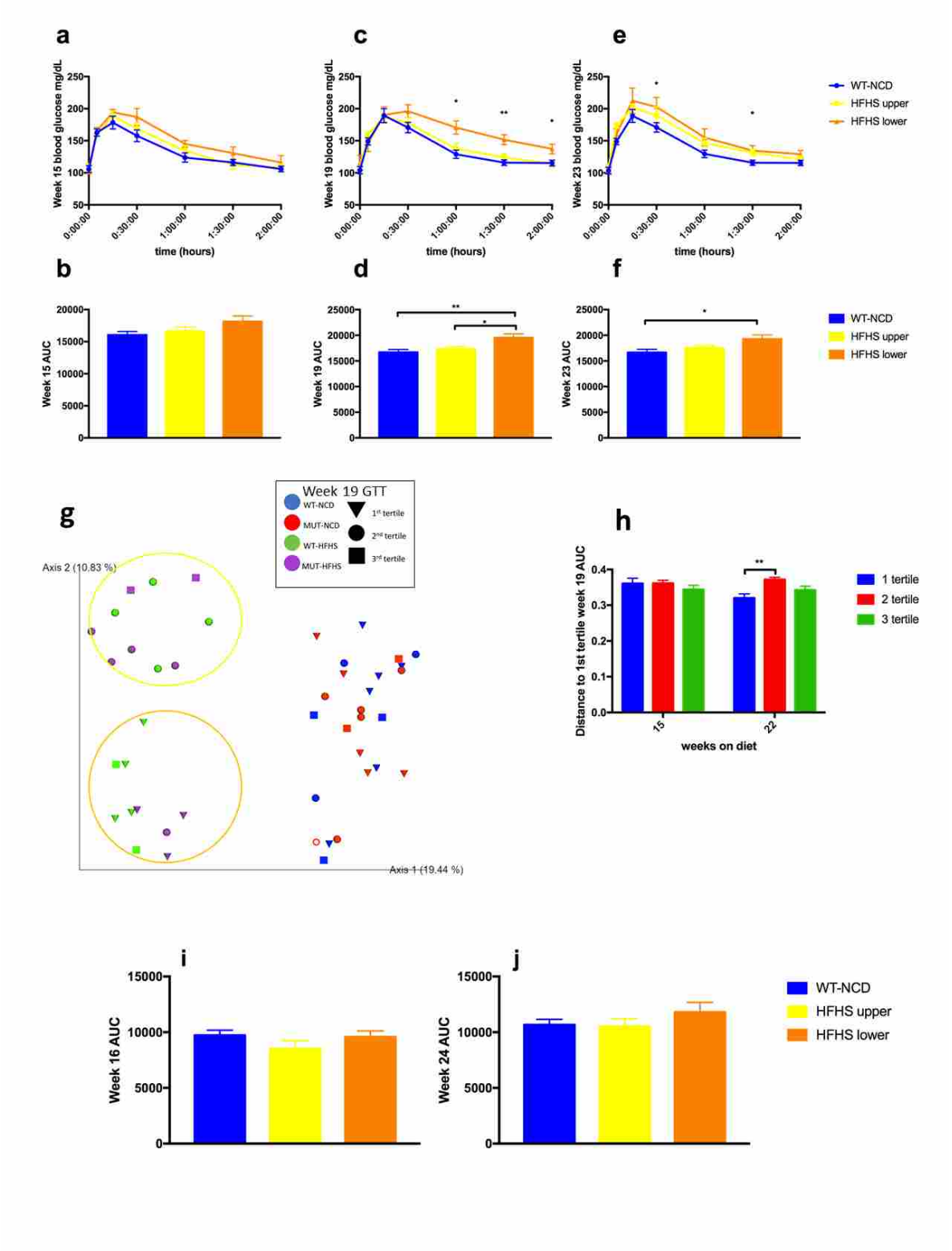

Figure 15. Gut microbial composition influences glucose response. (a) Week 15 GTT. (b) Week 15 AUC. (c) Week 19 GTT. (d) Week 19 AUC. (e) Week 23 GTT. (f) Week 23 AUC. (g) Unweighted UniFrac PCoA plot of week 22 samples coded by tertile of AUC by group. (h) Comparison of unweighted UniFrac distances of week 19 AUC tertile. (i) Week 16 ITT AUC (j) Week 24 ITT AUC.

To determine whether genotype played any role in the gut microbiota divergence, we compared glucose response by diet and genotype in the upper and lower clusters against WT-NCD mice. The lower cluster of MUT-HFHS showed the most consistent impaired glucose response (Figure 16) with the greatest differences seen after 19 weeks on the diet (Figure 16d) (p=0.02). No significant differences were seen in glucose response between the MUT-HFHS upper and MUT-HFHS lower groups after 15 weeks on the diet when WT-HFHS mice were included in an ANOVA analysis (Figure 16b) (p=0.0772). But when the MUT-HFHS upper and lower group were compared via Student's T-test, there were significant differences in AUC between the two groups at 15 weeks (p=0.0211). At week 19 both the MUT-HFHS lower group (p=0.05), and the WT-HFHS lower group (p=0.0487) had greater AUC when compared to the WT-NCD group. At the 23-week timepoint (Figure 16f), only the MUT-HFHS lower group was significantly different from the WT-NCD group (p=0.0488). These results suggest that the MUT-HFHS mice showed a greater susceptibility to the shift in the microbiota.

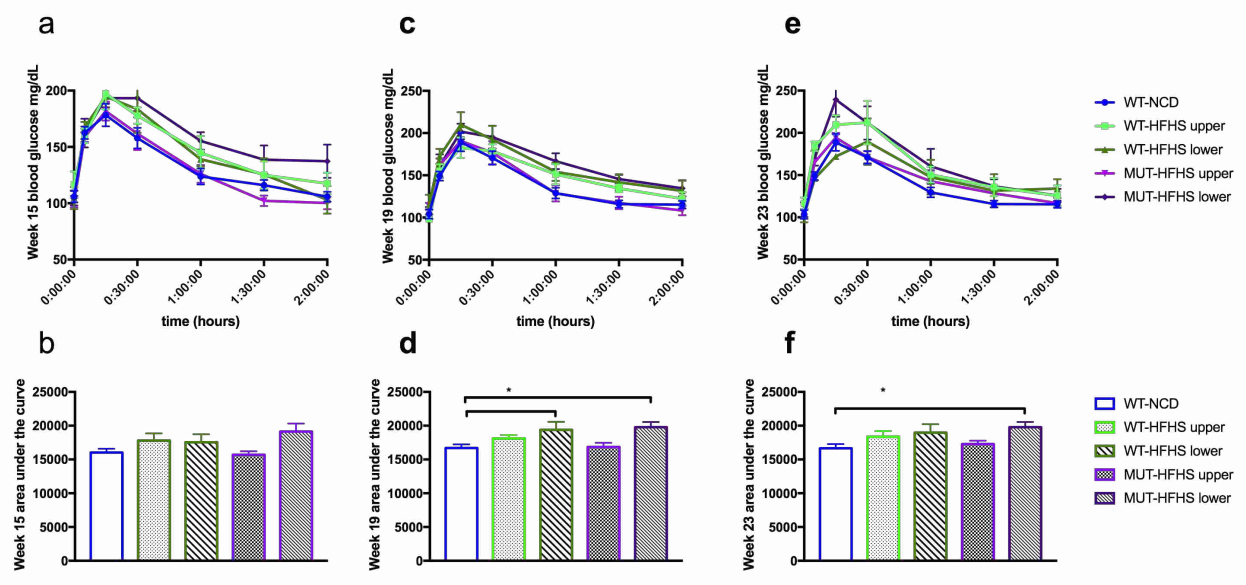

Figure 16. Genotype and microbial composition influences glucose response.(a) Week 15 GTT. (b) Week 15 GTT AUC. (c) Week 19 blood glucose. (d) Week 19 AUC. (e) Week 23 blood glucose. (f) Week 23 AUC.

Protein expression is linked to genotype and microbiota composition

To study the effect microbiota composition had on protein expression, we compared the upper and lower groups. A HFHS diet significantly decreased claudin-1 expression in both the upper and lower groups (Figure 17a). The HFHS lower cluster had considerably lower levels of claudin-1 compared to both the WT-NCD ($p<0.001$) and HFHS upper cluster ($p=0.0377$), suggesting a further deleterious effect provided by the microbiota in the lower cluster.

When separated by genotype, a HFHS diet significantly decreased claudin-1 expression in both the upper ($p=0.0012$) and lower ($p=0.0001$) WT groups and the MUT-HFHS lower group ($p=0.0453$) (Figure 17d) when compared to WT-NCD. Interestingly, however, the MUT-HFHS upper group showed claudin-1 levels similar to WT-NCD ($p=0.999$), suggesting a protective effect provided by deletion of PASK, which could be overcome by the microbiota in the lower cluster.

Akt expression showed no significant differences between any of the groups, regardless of diet, genotype, or microbiota clusters (Figure 17b and Figure 17e). Activated Akt (pAkt) expression did not differ by cluster (Figure 17c). When separated by genotype, pAkt was significantly elevated in the WT-HFHS lower group when compared to the MUT-HFHS lower group (Figure 17f) ($p=0.0026$). These results suggest that microbiota composition only affected claudin-1 expression.

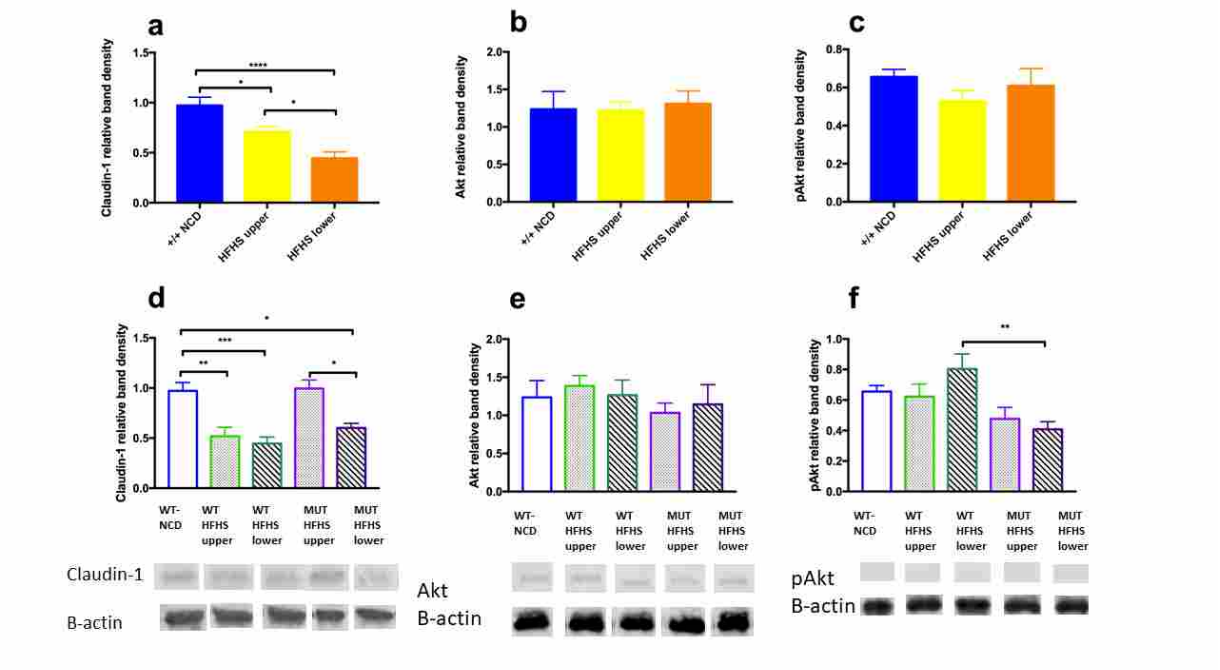

Figure 17. Microbiome influences changes in protein expression. (a)Comparison of relative expression of claudin-1 by unweighted UniFrac PCoA cluster. (b) Comparison of relative expression of Akt by unweighted UniFrac PCoA cluster. (c) Comparison of relative expression of pAkt by unweighted UniFrac PCoA cluster. (d) Comparison of relative expression of claudin-1 by unweighted UniFrac PCoA cluster and genotype. (e) Comparison of relative expression of Akt by unweighted UniFrac PCoA cluster and genotype. (f) Comparison of relative expression of pAkt by unweighted UniFrac PCoA cluster and genotype.

Discussion

Rates of obesity and insulin resistance in the United States are increasing, necessitating better animal models to better understand influencing factors. Deletion of PASK, a metabolic protein, has previously been shown to protect mice against high fat diet-induced weight gain and insulin resistance [47,50,53]. In the current study, we placed PASK mutant mice on a western-style HFHS diet rather than a high fat diet to examine its effects. Contrary to those previously published studies, deletion of PAS-kinase did not protect mice from weight gain on a western-style, HFHS diet. Deletion of PASK also failed to protect mice from glucose intolerance or insulin resistance. Mice of either genotype on the NCD, however, were protected from weight gain, glucose intolerance and insulin resistance, suggesting that diet played an overarching role in the development of poor metabolic health.

Both diet and genotype influenced expression of the tight-junction protein claudin-1. In wild type mice, the HFHS diet led to significantly less claudin-1 in the colon, whereas mutant mice were protected against a HFHS-induced claudin-1 decrease. Decreased levels of tight-junction proteins in the gut have been shown to correlate with increased gut permeability and systemic inflammation [25,34]. This result, therefore, suggests that even though PASK mutant mice were not protected against all of the harmful effects of the HFHS diet in this study (weight gain and glucose intolerance), they did show some metabolic advantages over wild type mice.

Diet was the only variable seen to contribute to differences in microbial composition between the groups, with the expected increases in *Firmicutes* and *Actinobacteria* seen in mice on the HFHS diet [7,67]. Genotype differences can influence microbiota composition. Unpublished research by our lab showed that deletion of CD5 significantly altered the gut microbiota in mice on NCD. Differences in gut microbiota were also seen in *p66Shc* $^{-/-}$ mice on a HFD [68]. However, in this study only diet correlated with composition of the gut microbiota.

One of the most interesting observations of this study was that within the HFHS mice of both genotypes, a spontaneous shift or split occurred in the gut microbiota composition. This split can be visualized in the unweighted UniFrac PCoA analysis shown in Fig. 14b. An examination of the mice in these two microbiota clusters revealed that none of the mice in the upper cluster were in the highest tertile of body weight. Mice in the lower microbiota cluster showed significantly poorer glucose tolerance after both 19 and 23 weeks on the HFHS diet, whereas mice in the upper microbiota cluster on the same diet showed a glucose response that was indistinguishable from that of wild type mice on a healthy NCD.

The cause of the divergence in microbiota composition between the two clusters in unknown, however maternal influences are unlikely due to the similarity of the HFHS microbiota at 15 weeks. All the mice were on the HFHS diet, and both clusters contained a mix of wild type and mutant mice. It is possible that the microbiota shift happened in some mice due to stress, which is a known disrupter of the gut microbiota [69]. This study extended across an 18-month window, and possible stressors include moving to a new building, building vibration due to neighboring construction projects, and many different experimenters and caretakers. Acute stress can also alter tight junction protein expression [70] [20], providing another potential explanation for the differences in claudin-1 expression.

A key observation of this study is that no gut microbiota divergence was detected in mice on the healthy NCD. This suggests that a healthy diet confers protection against potentially harmful disruptions to the gut microbiota, whereas the western-style diet left mice vulnerable to such disruption. Further studies controlling for stress as a variable, sequencing of additional timepoints between 15 and 22 weeks, and examining individual species and strains to determine which contributed to the harmful effects of the lower cluster gut microbiota may better explain the clustering seen in the HFHS mice.

In summary, we found that microbial differences, not the deletion of PASK, had the most profound influence on weight gain and glucose tolerance claudin-1in mice fed a high-fat diet. Our findings also showed that the best predictor of metabolic health was a NCD, illustrating the importance of diet on metabolic health.

Bibliography

1 Hales CM, C. M., Fryar CD, Ogden & Clarke, G. Prevalence of obesity among adults and youth: United States, 2015–2016., (National Center for Health Statistics, 2017).

2 The, G. B. D. O. C. *et al.* Global, regional and national prevalence of overweight and obesity in children and adults 1980-2013: A systematic analysis. *Lancet (London, England)* **384**, 766-781, doi:10.1016/S0140-6736(14)60460-8 (2014).

3 Alberti, K. G., Zimmet, P. & Shaw, J. The metabolic syndrome--a new worldwide definition. *Lancet (London, England)* **366**, 1059-1062, doi:10.1016/s0140-6736(05)67402-8 (2005).

4 Boulangé, C. L., Neves, A. L., Chilloux, J., Nicholson, J. K. & Dumas, M.-E. Impact of the gut microbiota on inflammation, obesity, and metabolic disease. *Genome Medicine* **8**, 42, doi:10.1186/s13073-016-0303-2 (2016).

5 Delzenne, N. M., Cani, P. D., Everard, A., Neyrinck, A. M. & Bindels, L. B. Gut microorganisms as promising targets for the management of type 2 diabetes. *Diabetologia* **58**, 2206-2217, doi:10.1007/s00125-015-3712-7 (2015).

6 Mahana, D. *et al.* Antibiotic perturbation of the murine gut microbiome enhances the adiposity, insulin resistance, and liver disease associated with high-fat diet. *Genome Medicine* **8**, 48, doi:10.1186/s13073-016-0297-9 (2016).

7 Moreno-Indias, I. *et al.* Insulin resistance is associated with specific gut microbiota in appendix samples from morbidly obese patients. *American journal of translational research* **8**, 5672-5684 (2016).

8 Kasuga, M., Karlsson, F. A. & Kahn, C. R. Insulin stimulates the phosphorylation of the 95,000-dalton subunit of its own receptor. *Science* **215**, 185-187 (1982).

9 Bryant, N. J., Govers, R. & James, D. E. Regulated transport of the glucose transporter GLUT4. *Nature reviews. Molecular cell biology* **3**, 267-277, doi:10.1038/nrm782 (2002).

10 Mokdad, A. H. *et al.* Prevalence of obesity, diabetes, and obesity-related health risk factors, 2001. *Jama* **289**, 76-79 (2003).

11 Mendola ND, C. T.-C., Gu Q, Eberhardt MS, Saydah S. Prevalence of total, diagnosed, and undiagnosed diabetes among adults: United States, 2013–2016. (National Center for Health Statistics 2018).

12 National Diabetes Statistics Report, 2017. (Centers for Disease Control and Prevention, U.S. Dept of Health and Human Services, Atlanta, GA, 2017).

13 Yang, Q. *et al.* Added sugar intake and cardiovascular diseases mortality among US adults. *JAMA internal medicine* **174**, 516-524, doi:10.1001/jamainternmed.2013.13563 (2014).

14 Stanhope, K. L. Sugar consumption, metabolic disease and obesity: The state of the controversy. *Critical reviews in clinical laboratory sciences* **53**, 52-67, doi:10.3109/10408363.2015.1084990 (2016).

15 Moreno, L. A. *et al.* Trends of Dietary Habits in Adolescents. *Critical Reviews in Food Science and Nutrition* **50**, 106-112, doi:10.1080/10408390903467480 (2010).

16 Fryar CD, H. J., Herrick KA, Ahluwalia, N. in. *NCHS Data Brief, no 322, National Center for Health Statistics* (Hyattsville, MD, 2018).

17 Qin, J. *et al.* A human gut microbial gene catalogue established by metagenomic sequencing. *Nature* **464**, 59-65, doi:10.1038/nature08821 (2010).

18 Sommer, F. & Bäckhed, F. Know your neighbor: Microbiota and host epithelial cells interact locally to control intestinal function and physiology. *BioEssays* **38**, 455-464, doi:doi:10.1002/bies.201500151 (2016).
19 Macfarlane, G. T. & Macfarlane, S. Fermentation in the human large intestine: its physiologic consequences and the potential contribution of prebiotics. *Journal of clinical gastroenterology* **45 Suppl**, S120-127, doi:10.1097/MCG.0b013e31822fecfe (2011).
20 Yan, H. & Ajuwon, K. M. Butyrate modifies intestinal barrier function in IPEC-J2 cells through a selective upregulation of tight junction proteins and activation of the Akt signaling pathway. *PloS one* **12**, e0179586, doi:10.1371/journal.pone.0179586 (2017).
21 Hooper, L. V., Littman, D. R. & Macpherson, A. J. Interactions between the microbiota and the immune system. *Science (New York, N.Y.)* **336**, 1268-1273, doi:10.1126/science.1223490 (2012).
22 Arpaia, N. *et al.* Metabolites produced by commensal bacteria promote peripheral regulatory T-cell generation. *Nature* **504**, 451-455, doi:10.1038/nature12726 (2013).
23 Grenham, S., Clarke, G., Cryan, J. F. & Dinan, T. G. Brain–Gut–Microbe Communication in Health and Disease. *Frontiers in Physiology* **2**, 94, doi:10.3389/fphys.2011.00094 (2011).
24 Ley, R. E. *et al.* Obesity alters gut microbial ecology. *Proceedings of the National Academy of Sciences of the United States of America* **102**, 11070-11075, doi:10.1073/pnas.0504978102 (2005).
25 Cani, P. D. *et al.* Changes in Gut Microbiota Control Metabolic Endotoxemia-Induced Inflammation in High-Fat Diet–Induced Obesity and Diabetes in Mice. *Diabetes* **57**, 1470-1481, doi:10.2337/db07-1403 (2008).
26 Bäckhed, F., Manchester, J. K., Semenkovich, C. F. & Gordon, J. I. Mechanisms underlying the resistance to diet-induced obesity in germ-free mice. *Proceedings of the National Academy of Sciences* **104**, 979-984, doi:10.1073/pnas.0605374104 (2007).
27 Fei, N. & Zhao, L. An opportunistic pathogen isolated from the gut of an obese human causes obesity in germfree mice. *The ISME journal* **7**, 880-884, doi:10.1038/ismej.2012.153 (2013).
28 Turnbaugh, P. J. *et al.* An obesity-associated gut microbiome with increased capacity for energy harvest. *Nature* **444**, 1027 (2006).
29 Shin, N.-R. *et al.* An increase in the Akkermansia spp. population induced by metformin treatment improves glucose homeostasis in diet-induced obese mice. *Gut* **63**, 727-735, doi:10.1136/gutjnl-2012-303839 (2014).
30 Zhao, L. *et al.* Gut bacteria selectively promoted by dietary fibers alleviate type 2 diabetes. *Science* **359**, 1151-1156, doi:10.1126/science.aao5774 (2018).
31 Everard, A. *et al.* Cross-talk between Akkermansia muciniphila and intestinal epithelium controls diet-induced obesity. *Proceedings of the National Academy of Sciences of the United States of America* **110**, 9066-9071, doi:10.1073/pnas.1219451110 (2013).
32 Karlsson, C. L. *et al.* The microbiota of the gut in preschool children with normal and excessive body weight. *Obesity (Silver Spring, Md.)* **20**, 2257-2261, doi:10.1038/oby.2012.110 (2012).
33 Backhed, F. *et al.* The gut microbiota as an environmental factor that regulates fat storage. *Proceedings of the National Academy of Sciences of the United States of America* **101**, 15718-15723, doi:10.1073/pnas.0407076101 (2004).

34 Martinez-Medina, M. *et al.* Western diet induces dysbiosis with increased E coli in CEABAC10 mice, alters host barrier function favouring AIEC colonisation. *Gut* **63**, 116-124, doi:10.1136/gutjnl-2012-304119 (2014).
35 Bergheim, I. *et al.* Antibiotics protect against fructose-induced hepatic lipid accumulation in mice: role of endotoxin. *Journal of hepatology* **48**, 983-992, doi:10.1016/j.jhep.2008.01.035 (2008).
36 Ashida, H., Ogawa, M., Kim, M., Mimuro, H. & Sasakawa, C. Bacteria and host interactions in the gut epithelial barrier. *Nature chemical biology* **8**, 36-45, doi:10.1038/nchembio.741 (2011).
37 Lim, S.-M., Jeong, J.-J., Woo, K. H., Han, M. J. & Kim, D.-H. Lactobacillus sakei OK67 ameliorates high-fat diet–induced blood glucose intolerance and obesity in mice by inhibiting gut microbiota lipopolysaccharide production and inducing colon tight junction protein expression. *Nutrition Research* **36**, 337-348 (2016).
38 Guo, S. *et al.* Lipopolysaccharide Regulation of Intestinal Tight Junction Permeability Is Mediated by TLR4 Signal Transduction Pathway Activation of FAK and MyD88. *The Journal of Immunology* **195**, 4999-5010, doi:10.4049/jimmunol.1402598 (2015).
39 Amar, J. *et al.* Intestinal mucosal adherence and translocation of commensal bacteria at the early onset of type 2 diabetes: molecular mechanisms and probiotic treatment. *EMBO Molecular Medicine* **3**, 559-572, doi:10.1002/emmm.201100159 (2011).
40 Wang, H. *et al.* l-Tryptophan Activates Mammalian Target of Rapamycin and Enhances Expression of Tight Junction Proteins in Intestinal Porcine Epithelial Cells. *The Journal of nutrition* **145**, 1156-1162, doi:10.3945/jn.114.209817 (2015).
41 Huang, X., Liu, G., Guo, J. & Su, Z. The PI3K/AKT pathway in obesity and type 2 diabetes. *International Journal of Biological Sciences* **14**, 1483-1496, doi:10.7150/ijbs.27173 (2018).
42 Alessi, D. R. *et al.* Characterization of a 3-phosphoinositide-dependent protein kinase which phosphorylates and activates protein kinase Balpha. *Current biology : CB* **7**, 261-269 (1997).
43 Liu, P. *et al.* PtdIns(3,4,5)P3-Dependent Activation of the mTORC2 Kinase Complex. *Cancer discovery* **5**, 1194-1209, doi:10.1158/2159-8290.cd-15-0460 (2015).
44 Bagarolli, R. A. *et al.* Probiotics modulate gut microbiota and improve insulin sensitivity in DIO mice. *The Journal of nutritional biochemistry* **50**, 16-25, doi:10.1016/j.jnutbio.2017.08.006 (2017).
45 Gao, Z. *et al.* Butyrate Improves Insulin Sensitivity and Increases Energy Expenditure in Mice. *Diabetes* **58**, 1509-1517, doi:10.2337/db08-1637 (2009).
46 Liu, Y. *et al.* A high sucrose and high fat diet induced the development of insulin resistance in the skeletal muscle of Bama miniature pigs through the Akt/GLUT4 pathway. *Experimental Animals* **66**, 387-395, doi:10.1538/expanim.17-0010 (2017).
47 Perez-Garcia, A. *et al.* High-fat diet alters PAS kinase regulation by fasting and feeding in liver. *The Journal of nutritional biochemistry* **57**, 14-25, doi:10.1016/j.jnutbio.2018.03.003 (2018).
48 Pérez-García, A. *et al.* PAS Kinase deficiency alters the glucokinase function and hepatic metabolism. *Scientific reports* **8**, 11091-11091, doi:10.1038/s41598-018-29234-8 (2018).
49 Rutter, J., Michnoff, C. H., Harper, S. M., Gardner, K. H. & McKnight, S. L. PAS kinase: An evolutionarily conserved PAS domain-regulated serine/threonine kinase. *Proceedings*

of the National Academy of Sciences **98**, 8991-8996, doi:10.1073/pnas.161284798 (2001).
50 da Silva Xavier, G. *et al.* Per-arnt-sim (PAS) domain-containing protein kinase is downregulated in human islets in type 2 diabetes and regulates glucagon secretion. *Diabetologia* **54**, 819-827, doi:10.1007/s00125-010-2010-7 (2011).
51 Zhang, D. D. *et al.* Per-Arnt-Sim Kinase (PASK): An Emerging Regulator of Mammalian Glucose and Lipid Metabolism. *Nutrients* **7**, 7437-7450, doi:10.3390/nu7095347 (2015).
52 DeMille, D. & Grose, J. H. PAS kinase: a nutrient sensing regulator of glucose homeostasis. *IUBMB life* **65**, 921-929, doi:10.1002/iub.1219 (2013).
53 Hao, H.-X. *et al.* PAS kinase is required for normal cellular energy balance. *Proceedings of the National Academy of Sciences of the United States of America* **104**, 15466-15471, doi:10.1073/pnas.0705407104 (2007).
54 Godon, J. J., Zumstein, E., Dabert, P., Habouzit, F. & Moletta, R. Molecular microbial diversity of an anaerobic digestor as determined by small-subunit rDNA sequence analysis. *Applied and environmental microbiology* **63**, 2802-2813 (1997).
55 Caporaso, J. G. *et al.* QIIME allows analysis of high-throughput community sequencing data. *Nature methods* **7**, 335-336, doi:10.1038/nmeth.f.303 (2010).
56 Callahan, B. J. *et al.* DADA2: High-resolution sample inference from Illumina amplicon data. *Nature methods* **13**, 581-583, doi:10.1038/nmeth.3869 (2016).
57 McDonald, D. *et al.* The Biological Observation Matrix (BIOM) format or: how I learned to stop worrying and love the ome-ome. *GigaScience* **1**, 7, doi:10.1186/2047-217x-1-7 (2012).
58 Bokulich, N. A. *et al.* Optimizing taxonomic classification of marker-gene amplicon sequences with QIIME 2's q2-feature-classifier plugin. *Microbiome* **6**, 90, doi:10.1186/s40168-018-0470-z (2018).
59 Pedregosa, F. *et al.* Scikit-learn: Machine Learning in Python. *Journal of Machine Learning Research* **12**, 2825-2830 (2011).
60 Vazquez-Baeza, Y., Pirrung, M., Gonzalez, A. & Knight, R. EMPeror: a tool for visualizing high-throughput microbial community data. *GigaScience* **2**, 16, doi:10.1186/2047-217x-2-16 (2013).
61 Vazquez-Baeza, Y. *et al.* Bringing the Dynamic Microbiome to Life with Animations. *Cell Host Microbe* **21**, 7-10, doi:10.1016/j.chom.2016.12.009 (2017).
62 Anderson, M. J. A new method for non-parametric multivariate analysis of variance. *Austral Ecology* **26**, 32-46, doi:10.1046/j.1442-9993.2001.01070.x (2001).
63 Kruskal, W. H. & Wallis, W. A. USE OF RANKS IN ONE-CRITERION VARIANCE ANALYSIS. *Journal of the American Statistical Association* **47**, 583-621 (1952).
64 Faith, D. P. Conservation evaluation and phylogenetic diversity. *Biological Conservation* **61**, 1-10 (1992).
65 Bokulich, N. A. *et al.* Optimizing taxonomic classification of marker-gene amplicon sequences with QIIME 2's q2-feature-classifier plugin. *Microbiome* **6**, 90, doi:10.1186/s40168-018-0470-z (2018).
66 Lozupone, C. & Knight, R. UniFrac: a new phylogenetic method for comparing microbial communities. *Applied and environmental microbiology* **71**, 8228-8235, doi:10.1128/aem.71.12.8228-8235.2005 (2005).
67 Carvalho, B. M. *et al.* Modulation of gut microbiota by antibiotics improves insulin signalling in high-fat fed mice. *Diabetologia* **55**, 2823-2834, doi:10.1007/s00125-012-2648-4 (2012).
68 Ciciliot, S. *et al.* Interplay between gut microbiota and p66Shc affects obesity-associated insulin resistance. *FASEB journal : official publication of the Federation of American Societies for Experimental Biology* **32**, 4004-4015, doi:10.1096/fj.201701409R (2018).

69 Bridgewater, L. C. *et al.* Gender-based differences in host behavior and gut microbiota composition in response to high fat diet and stress in a mouse model. *Sci Rep* **7**, 10776, doi:10.1038/s41598-017-11069-4 (2017).

70 Demaude, J., Salvador-Cartier, C., Fioramonti, J., Ferrier, L. & Bueno, L. Phenotypic changes in colonocytes following acute stress or activation of mast cells in mice: implications for delayed epithelial barrier dysfunction. *Gut* **55**, 655-661, doi:10.1136/gut.2005.078675 (2006).